Methods used in Klimaatlas, the Danish Climate Atlas (v2024b)

DMI Report 24-12

National Centre for Climate Research (NCKF) at DMI

13 November 2024

National Centre for Climate Research (NCKF) at DMI

Danish Meteorological Institute

Colophon

Serial title	DMI Report
Title	Methods used in Klimaatlas, the Danish Climate Atlas (v2024b)
Report Number	DMI Report 24-12
Author(s)	National Centre for Climate Research (NCKF) at DMI
Editor	Peter Thejil
Language	English
Keywords	Climate change, Klimaatlas
URL	https://www.dmi.dk/klimaatlas/
Digital ISBN	978-87-7478-755-6
Version	v2024b
Version date	13 November 2024
Copyright	Danish Meterological Insitute
Citation	This report should be cited as: DMI (2024).Methods used in Klimaatlas, the Danish Climate Atlas (v2024b). DMI Report 24-12. https://doi.org/10.5281/zenodo.13753022 Klimaatlas data should be cited as: DMI. (2024). DMI Klimaatlas v2024b - Fremskrivninger af det danske klima (Projections of climate indicators in Denmark) [Data set]. Zenodo. https://doi.org/10.5281/zenodo.13753022

Danish Meteorological Institute

Table of Contents

Changes in this version

Klimaatlas v2024b represents a significant update of indicators associated with sea level rise and storm surges in Denmark. The release updates existing storm surge indicators based on upon new data (*Højvandsstatistikker*) from *Kystdirektoratet* released in July 2024 and updated again in November 2024. In addition, a rewrite of the sea-level and storm-surge processing code has aligned this part of the pipeline with the rest of the *Klimaatlas* processing chain. The resulting changes in indicators are generally minor, and within the uncertainty associated with estimates: notable changes may occur in some instances and are highlighted below.

In addition, the number of emissions scenarios available for sea-level rise and storm-surge indicators has been increased. This reflects the increasing focus on scenarios beyond the core set previously used in *Klimaatlas*, and particularly on SSP3-7.0.

Sea Level Rise and Storm Surge Statistics

Input data

- **Update of *Højvandsstatistikker* from 2017 to 2024 version**. There is generally good agreement between the resulting storm-surge indicators, with revisions generally being minor.
  Impacted indicators: 202-204, 206, 208, and 210.

- **Use of land-rise rates as reported in *Højvandsstatistikker***, rather than from the source report from DTU as done previously. This change ensures coherency between *Højvandsstatistikker* and *Klimaatlas*.
  Impacted indicators: all sea-level and storm surge indicators (201-204, 206, 208, 210, 213).

- **Improved utilization of sea-level rise projections from IPCC AR6**. Previous versions of *Klimaatlas* built upon a simplified version of the available sea-level rise projections as inputs that required the uncertainties of interest (10th and 90th percentiles) to be inferred from the data available (83rd and 95th percentiles). v2024b uses the full set of sea-level rise projection data, allowing the relevant uncertainties to be extracted directly.
  Impacted indicators: all sea-level and storm surge indicators (201-204, 206, 208, 210, 213).

Methods

- The **reference year for sea-level rise** calculations has been moved to 1995, whereas it was previously 1990. This change resolves a minor inconsistency between the choice of reference year and the average sea level rise over the historical period. The resulting net change in sea level indicators is less than 2cm averaged across all stations.
  Impacted indicators: all sea-level and storm surge indicators (201-204, 206, 208, 210, 213).

- **Removal of DKSS storm-surge model based variance contributions**. The calculation of future storm-surge indicators in Klimaatlas previously used a limited set of simulations using the DKSS storm surge model under two RCPs to estimate uncertainties in future storm surges associated with changes in wind patterns. However, while v2024b now presents five SSP-based emissions scenarios for sea-level rise and storm-surges, there are no corresponding SSP-based simulations available using the DKSS model system. The use of DKSS simulations in estimating the variance of future storm surge statistics has therefore been discontinued. The impact on the indicators is minor.

Impacted indicators: all storm surge indicators (202-204, 206, 208, 210, 213).

- **Rewrite of the calculation** of sea-level rise and storm-surge indicators using Python. Agreement between indicators calculated with the old and new code with the same input data was generally excellent.
  Impacted indicators: all sea-level and storm surge indicators (201-204, 206, 208, 210, 213).

Indicators

- **Addition of a new indicator (213)**, frequency with which the current 100 year storm surge level will be exceeded in the future.

- **Removal of indicator 205** (height of 10 000 year storm surge). Recent work in relation to the protection of Copenhagen against storm surges concluded that the use of statistical extrapolation to such long return periods was not supported by the (comparatively short-duration) time series available (Su et al 2024). This indicator has therefore been removed. The last published version of this indicator can be found in the *Klimaatlas* archive in version v2024a:
  https://zenodo.org/doi/10.5281/zenodo.11402835

- **Suspension of indicator 211** (Frequency of storm surge events exceeding current local warning level). Indicator 211 was previously calculated on the basis of DKSS simulations and cannot therefore be calculated as previously. A new calculation method, similar to that used for 210 and 213 is being developed, and indicator 211 has therefore been suspended for the meantime. A new version of the indicator will be released in a future update. The last published version of this indicator can be found in the *Klimaatlas* archive in version v2024a: https://zenodo.org/doi/10.5281/zenodo.11402835

- **Removal of indicator 212** (Accumulated duration of sea level exceeding current local warning level). Together with indicator 211, this indicator was previously calculated based on a limited set of DKSS model runs. It was not possible to find a new method to calculate this indicator with the new set of scenarios and it has therefore been removed. The last published version of this indicator can be found in the *Klimaatlas* archive in version v2024a: https://zenodo.org/doi/10.5281/zenodo.11402835

- **Indicator 210 shows the greatest change** as a result of the above changes to methods and input data. Indicator 210 describes the frequency with which the level of a 20-year storm-surge in the current climate will be exceeded in the future and therefore integrates both changes in storm-surge statistics and sea level rise. The agreement between v2024b and v2024a is however good (R^2 between v2024a and v2024b = 0.79, mean difference between v2024a and v2024b = 0.4 events per 20 years).

Webpage and Documentation

- **Addition of extra SSP scenarios and time periods** to the map viewer for sea level rise and storm surge statistics. Previously only three SSP scenarios were presented in the core *Klimaatlas* products (SSP1-2.6, SSP2-4.5 and SSP5-8.5), covering the last two periods (2041-2070 and 2071-2100). In line with the increased focus that SSP3-7.0 is receiving in an adaptation context, the set of scenarios has now been extended to include all five major SSP scenarios (i.e. addition of SSP3-7.0 and SSP1-1.9). Furthermore, the removal of DKSS data from the processing pipeline now makes it possible to generate *Kommune* reports and excel spreadsheets have also been updated accordingly.

Other Changes

Input data

- **Two additional atmospheric models** that were previously excluded from calculations involving Tmax and Tmin have been incorporated into *Klimaatlas*, increasing the ensemble size for indicators derived from these two variables. While there are subsequent revisions to estimates of both the median and the uncertainties, the changes are generally minor.

  Impacted indicators: 002-005,007-010

1. Introduction

Klimaatlas, the Danish National Climate Atlas, provides Danish society with relevant and easy to-use information on expected future changes in climate, including changes in atmospheric temperatures, precipitation and derived indices, as well as from the sea surrounding Denmark (sea-level and storm surges).

Klimaatlas is based primarily on regional climate models derived from the EURO-CORDEX archives [Jacob et al., 2014], (https://euro-cordex. net/). However, such model data must be adjusted or calibrated so that they represent the current climate correctly. Observational data therefore also plays a key role in the production of *Klimaatlas* outputs – a significant amount of the work performed in the development of *Klimaatlas* is focused on ensuring harmony between these two data sources.

Klimaatlas products are provided in several data-formats – .xlsx spreadsheets, .netcdf files and as ’GIS layers’. This data is intended for users requiring download of material for further processing, but *Klimaatlas* also provides an online display of the information, with documentation and user guides. Furthermore, reports are generated for each of the 98 *kommuner* (municipalities) in Denmark, summarizing the key findings from Klimaatlas, together with a report covering the entire country.

Each indicator describes absolute values as well as changes in the index, expressed in percent or physical units as appropriate. Information, except the ocean indices, is available on a 1x1 km grid as well as on an aggregated basis for municipalities and main catchment areas. The ocean indices are available on 34 coastal stretches. Information is made available for the four seasons (and an annual value) for multiple emission scenarios. Four time periods are used - a present-day reference period (1981-2010) and three future periods (near future 2011-2040, mid-century 2041-2070, and end of century 2071-2100).

Klimaatlas is available online at http://www.dmi.dk/klimaatlas and is accompanied by detailed help and user-information. *Klimaatlas* was launched on 6th October 2019 and has been updated frequently since. An overview of the different versions can be found in “Appendix A Previous versions”.

This Technical Report describes the data processing leading to the results displayed. Where appropriate, justification for the choices made is provided and elaborated as necessary. The report is made up of several sections, and reading each in isolation should be possible.

2. Input data

2.1. Definitions

As a first step, we define two types of data that we deal with in *Klimaatlas*.

- *Climate variable* We refer to gridded climate data in its native time resolution as a "climate variable". This can include the output produced directly by a climate model (either global or regional) or observations. It can also include derived variables, that are produced as a combination of other variables from the same data source, or in interaction with other data sources (e.g. as in bias correction). Examples include temperature, maximum temperature, and precipitation.

- *Climate indicator* Climate variables can then be translated into climate indicators via a processing scheme involving the generation of some form of summary statistic (e.g. a mean) over time. Examples include annual mean temperature, frequency of extreme rain events, and drought indices.

The key distinction between a variable and an indicator is the act of time-averaging. Climate variables have a higher time resolution (e.g. months, days or hours) than the corresponding indicators (e.g. annual averages, 30 year averages). The information delivered by a climate service, including *Klimaatlas*, and that commonly serves as the basis for further decision making, is most commonly in the form of "indicators". Climate variables, however, are the precursor for indicators and often an intermediate step in the processing chain.

2.2. EURO-CORDEX model data

The models we use from the CORDEX archive is a subset of what is available. In particular, we note the following changes:

- CNRM version 1 models used the incorrect boundary forcing and were excluded.

- Despite using a differently rotated grid, the Aladin regional climate model has been re-gridded to the EUR-11 standard grid, and is used.

The final list of models used in Klimaatlas is given in Table 1.

#	GCM	RCM	member	tas	tasmax	tasmin	pr	pr1h	sfcWind	sfcWindmax	rsds	hurs
1	CANESM	CCLM	r1i1p1	h8	h8	h8	h8	h8	h8		h8	h8
2	CANESM	REMO15	r1i1p1	h8	h8	h8	h8	h8	h8	h8	h8	
3	CNRM	crCLIM	r1i1p1	h8	h8	h8	h8	h8	h8	h8	h8	h8
4	CNRM	ALADIN	r1i1p1	h48	h48	h48	h48	h48	h48	h48	h48	
5	CNRM	HIRHAM	r1i1p1	h8	h8	h8	h8	h8	h8	h8	h8	h8
6	CNRM	REMO15	r1i1p1	h28	h28	h28	h28	h28	h28	h28	h28	h28
7	CNRM	REGCM	r1i1p1	h8	h8	h8	h8	h8	h8	h8	h8	h8
8	CNRM	WRF381	r1i1p1	h8	h8	h8	h8		h8	h8	h8	
9	CNRM	RACMO	r1i1p1	h248	h248	h248	h248		h248	h248	h248	h248
10	CNRM	HADREM	r1i1p1	h8	h8	h8	h8	h8	h8	h8	h8	h8
11	ECEARTH	crCLIM	r1i1p1	h8	h8	h8	h8	h8	h8	h8	h8	h8
12	ECEARTH	HIRHAM	r1i1p1	h8	h8	h8	h8	h8	h8	h8	h8	h8
13	ECEARTH	RACMO	r1i1p1	h48	h48	h48	h48	h48	h48	h48	h48	h48
14	ECEARTH	RCA	r1i1p1	h8	h8	h8	h8	h8	h8	h8	h8	h8
15	ECEARTH	WRF361	r1i1p1	h8			h8				h8	
16	ECEARTH	crCLIM	r3i1p1	h8	h8	h8	h8	h8	h8	h8	h8	h8
17	ECEARTH	HIRHAM	r3i1p1	h248	h248	h248	h248	h248	h248	h248	h248	h248
18	ECEARTH	RACMO	r3i1p1	h8	h8	h8	h8		h8	h8	h8	h8
19	ECEARTH	RCA	r3i1p1	h8	h8	h8	h8	h8	h8	h8	h8	h8
20	ECEARTH	CCLM	r12i1p1	h248	h248	h248	h248		h248	h248	h248	
21	ECEARTH	crCLIM	r12i1p1	h8	h8	h8	h8	h8	h8	h8	h8	h8
22	ECEARTH	HIRHAM	r12i1p1	h8	h8	h8	h8	h8	h8	h8	h8	h8
23	ECEARTH	REMO15	r12i1p1	h248	h248	h248	h248	h48	h248	h248	h248	

#	GCM	RCM	member	tas	tasmax	tasmin	pr	pr1h	sfcWind	sfcWindmax	rsds	hurs
24	ECEARTH	REGCM	r12i1p1	h8	h8	h8	h8	h8	h8	h8	h8	h8
25	ECEARTH	WRF381	r12i1p1	h8	h8	h8	h8		h8	h8	h8	h8
26	ECEARTH	RACMO	r12i1p1	h248	h248	h248	h248		h248	h248	h248	h248
27	ECEARTH	HADREM	r12i1p1	h28	h28	h28	h28	h28	h28	h28	h28	h28
28	ECEARTH	RCA	r12i1p1	h248	h248	h248	h248	h248	h248	h248	h248	h248
29	ECEARTH	WRF361	r12i1p1	h8	h8	h8	h8		h8			
30	HADGEM	CCLM	r1i1p1	h48	h48	h48	h48		h48	h48	h48	
31	HADGEM	crCLIM	r1i1p1	h8	h8	h8	h8	h8	h8	h8	h8	h8
32	HADGEM	ALADIN	r1i1p1	h8	h8	h8	h8	h8	h8	h8	h8	
33	HADGEM	HIRHAM	r1i1p1	h248	h248	h248	h248	h248	h248	h248	h248	h248
34	HADGEM	REMO15	r1i1p1	h248	h248	h248	h248	h48	h248	h248	h248	
35	HADGEM	REGCM	r1i1p1	h28	h28	h28	h28		h28	h28	h28	h28
36	HADGEM	WRF381	r1i1p1	h8	h8	h8	h8		h8	h8	h8	
37	HADGEM	HADREM	r1i1p1	h28	h28	h28	h28	h28	h28	h28	h28	h28
38	HADGEM	RACMO	r1i1p1	h248	h248	h248	h248	h48	h248	h248	h248	h248
39	HADGEM	RCA	r1i1p1	h248	h248	h248	h248	h248	h248	h248	h248	h248
40	HADGEM	WRF361	r1i1p1	h8	h8	h8	h8		h8		h8	
41	IPSL	HIRHAM	r1i1p1	h8	h8	h8	h8	h8	h8	h8	h8	h8
42	IPSL	REMO15	r1i1p1	h8	h8	h8	h8	h8	h8	h8	h8	h8
43	IPSL	WRF381	r1i1p1	h48	h48	h48	h48		h48	h48	h48	
44	IPSL	RACMO	r1i1p1	h8	h8	h8	h8		h8	h8	h8	h8
45	IPSL	RCA	r1i1p1	h48	h48	h48	h48	h48	h48	h48	h48	h48
46	MIROC	CCLM	r1i1p1	h28	h28	h28	h28	h8	h28		h28	h8
47	MIROC	REMO15	r1i1p1	h28	h28	h28	h28	h8	h28	h28	h28	
48	MIROC	WRF361	r1i1p1	h8			h8		h8		h8	
49	MPI	CCLM	r1i1p1	h248	h248	h248	h248	h8	h248	h248	h248	
50	MPI	crCLIM	r1i1p1	h8	h8	h8	h8	h8	h8	h8	h8	h8
51	MPI	HIRHAM	r1i1p1	h8	h8	h8	h8	h8	h8	h8	h8	h8
52	MPI	REGCM	r1i1p1	h28	h28	h28	h28	h28	h28	h28	h28	h28
53	MPI	WRF381	r1i1p1	h8	h8	h8	h8		h8	h8	h8	h8
54	MPI	RACMO	r1i1p1	h28	h28	h28	h28		h28	h28	h28	h28
55	MPI	HADREM	r1i1p1	h8	h8	h8	h8	h8	h8	h8	h8	h8
56	MPI	REMO09	r1i1p1	h248	h248	h248	h248	h48	h248	h248	h248	
57	MPI	RCA	r1i1p1	h248	h248	h248	h248	h248	h248	h248	h248	h248
58	MPI	WRF361	r1i1p1	h28	h28	h28	h28		h28		h28	
59	MPI	crCLIM	r2i1p1	h8	h8	h8	h8	h8	h8	h8	h8	h8
60	MPI	REMO09	r2i1p1	h248	h248	h248	h248	h48	h248	h248	h248	
61	MPI	RCA	r2i1p1	h8	h8	h8	h8	h8	h8	h8	h8	h8
62	MPI	crCLIM	r3i1p1	h8	h8	h8	h8	h8	h8	h8	h8	h8
63	MPI	REMO15	r3i1p1	h8	h8	h8	h8	h8	h8	h8	h8	h8
64	MPI	RCA	r3i1p1	h8	h8	h8	h8	h8	h8	h8	h8	h8
65	NORESM	crCLIM	r1i1p1	h8	h8	h8	h8	h8	h8	h8	h8	h8
66	NORESM	HIRHAM	r1i1p1	h48	h48	h48	h48	h48	h48	h48	h48	h48
67	NORESM	REMO15	r1i1p1	h248	h248	h248	h248	h248	h248	h248	h248	h248
68	NORESM	REGCM	r1i1p1	h28	h28	h28	h28	h28	h28	h28	h28	h28
69	NORESM	WRF381	r1i1p1	h8	h8	h8	h8		h8	h8	h8	
70	NORESM	HADREM	r1i1p1	h8	h8	h8	h8	h8	h8	h8	h8	h8
71	NORESM	RACMO	r1i1p1	h28	h28	h28	h28		h28	h28	h28	h28
72	NORESM	RCA	r1i1p1	h248	h248	h248	h248	h248	h248	h248	h248	h248

Table 1 List of the climate model simulations used for the climate indices produced within *Klimaatlas*. Each row represents one model simulation with a forcing global climate model (GCM), a downscaling regional climate model (RCM) and a realisation identifier. Columns represent one variable used – see Table 2 for an explanation of variable codes. For each variable and model simulation we denote the scenarios available by h (historical period), 2 (RCP2.6), 4 (RCP4.5) and 8 (RCP8.5).

2.3. Observational data

The Danish Meteorological Institute (DMI) operates measurement stations for temperature, precipitation, and other observables across Denmark. The observational data were used to produce evenly-spaced grids of data (10x10 km for precipitation, and 20x20 km for temperature) called ’Klimagrid Danmark’ (KGDK) [Scharling, 1999, 2012, Wang and Scharling, 2012]. The grid used in KGDK is locked to the ’det Danske kvadratnet’ grid [Danmarks Statistik, 2019] (Figure 1).

It should be noted that, in order to match DMI official climate normals for mean precipitation, KGDK precipitation data was used that is not corrected for undercatch.

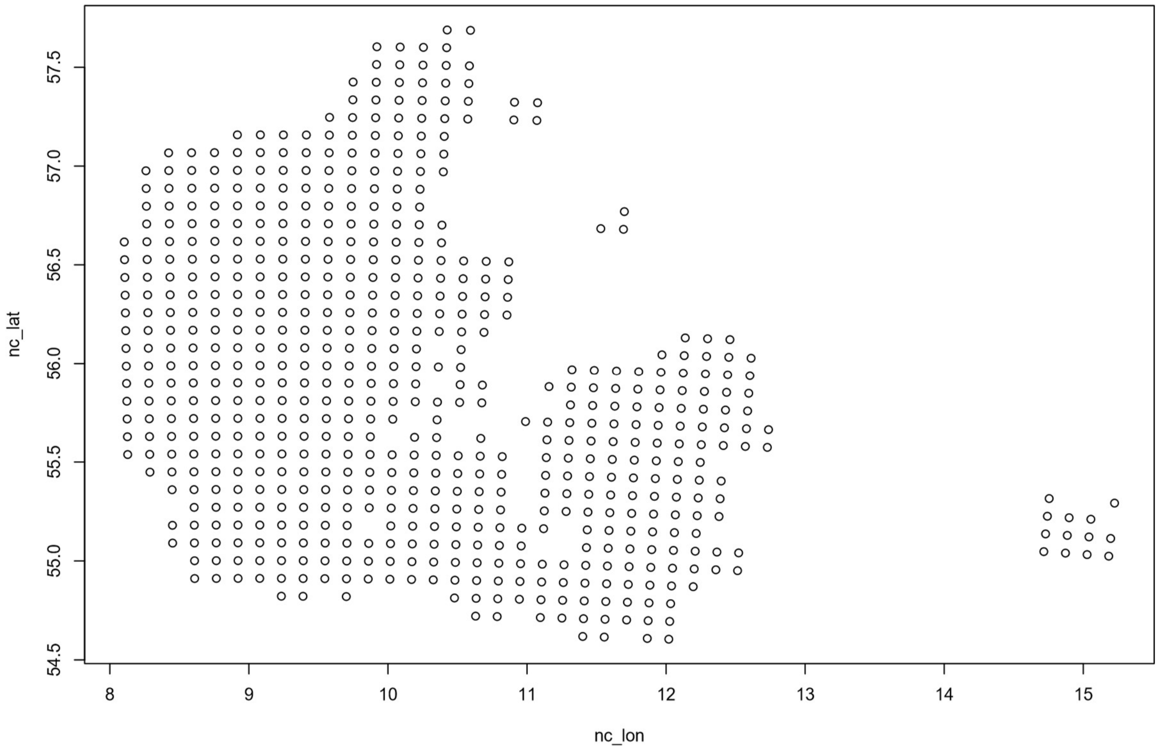

Figure 1. The Klimagrid Danmark grid for precipitation. Note that both Anholt and Læsø are represented.

For each climate variable selected from the EURO-CORDEX ensemble (see Table 1), a corresponding observational data product was obtained to serve as the basis for bias correction and calibration (Table 2).

ClimateVariable(s)		Observational Data Source
Code	Name	
tas	Daily mean temperature	KGDK, 20x20km, Daily mean, 1989-2019
tasmax	Daily maximum temperature	KGDK, 10x10km, Daily mean, 2011-2019
tasmin	Daily minimum temperature	KGDK, 10x10km, Daily mean, 2011-2019
pr	Daily total precipitation amount	KGDK, 10x10km, Daily mean, 2004-2019
pr1hr	Hourly total precipitation amount	No directly comparable product availabe
sfcWind	Daily mean wind speed	KGDK, 20x20km, Daily mean, 1989-2019
sfcWindMax	Daily maximum wind speed	KGDK, 20x20km, Daily mean, 2011-2019
rsds	Daily mean downward shortwave radiation	KGDK, 20x20km, Daily mean, 1989-2019
hurs	Relative humidity	
potevap	Potential evaporation	KGDK, 20x20km, Daily mean, 1989-2019

Table 2 Observational data used for the various climate variables in *Klimaatlas*.

3. Model calibration techniques

Model calibration essentially deals with the reality that distributions of climate model data are not usually identical to distributions of the same quantities observed. The differences can lie in different mean values, or, usually, in distributions that neither have the same mean nor the same shape (widths, for instance). Methods that deal with the task of making model data distributions more or less similar to observed data, are here generally termed "calibration" methods, with additional nomenclature to indicate precisely which form of adjustment is used. These concepts will be discussed below.

Calibration methods can be quite different, as we shall see, based on which variable considered. Common to them all is that they are based on somehow using information taken from the observational world. An issue arises if the observational data are not very extensive, so each method may have to be adapted to the particulars of the situation.

In climate-change work a ’reference period’ is often employed, such as 1986-2005 in IPCC AR5 and 1995-2014 in IPCC AR6, as a baseline to calculate climate change. The beginning and length of this period are typically carefully chosen in order to achieve a number of things. One goal is to help diminish the influence of natural variability – i.e. the reference period should be long enough to smooth out variations, but not so long it extends over important phases of climate change. We have here chosen as ’reference period’ 1981-2010 which is a compromise to have a period as close to present as possible, 30 years long, and to symmetrically overlap the AR5 reference period.

A ’calibration period’ is also chosen, which is the period during which observed and model data both exist. The calibration period is used to determine the data transformations required. This period may be different for different climate variables due to observational constraints.

As is the norm in climate work, statements about future expected climate change are often made in terms of the change between two periods – one will then typically be the reference period while the other is some ’future period’ such as 2011-2040, 2041-2070, and 2071-2100 (these will be used in *Klimaatlas*, see Figure 2). For example, precipitation-change is quantified in terms of a ratio, while for temperature it is given as a difference.

In *Klimaatlas*, two different families of calibration methods are applied. This first method focuses on the calibration of the core and shoulders of the distribution (i.e. the non-extreme parts), while the second focuses on the calibration of extremes. A significant amount of work was performed in the establishment of *Klimaatlas* to investigate the choice of calibration method within each of these use cases. In the interests of brevity, the work is not reproduced here but the reader is instead referred to the following publications:

- For choice of calibration methods for non-extreme parts of the distribution,
    - see Section 3 in DMI Report 24-11 .
- For the choice of calibrations methods for extremes,
    - Section 4 in DMI Report 24-11
    - [Schmith et al., 2023].

The following section describes how model calibration is currently implemented in *Klimaatlas*.

3.1. Quantile-Quantile Matching

The quantile-quantile matching method is used in *Klimaatlas* for calibration of the core and shoulders of a climate variables distribution. Extreme values associated with the calibrated distribution are not viewed as reliable and other techniques are therefore used in this case (see Section 3.1.5).

3.1.1. Nomenclature

Figure 2 explains some of the nomenclature used in this report. A model variable is denoted M.

The different periods are indicated with sub-scripts: M_c, M_r, and M_f refer to model values in the calibration period, the reference period, and the future period, respectively. In the calibration period we have simultaneous values of the model M_c and observations O. The calibrated model values in the reference period and the future period are denoted $\tilde{M}_r$, and $\tilde{M}_f$.

There are two over-arching types of calibration methods. The first type is denoted δ-change and is based on a mapping $M_c \rightarrow M_f$. This mapping is then applied to O to get $\tilde{M}_f$: $O \rightarrow \tilde{M}_f$. The other method is known as bias correction. This is based on a mapping $M_c \rightarrow O$ which is then applied to M_f to get $\tilde{M}_f$: $M_f \rightarrow \tilde{M}_f$.

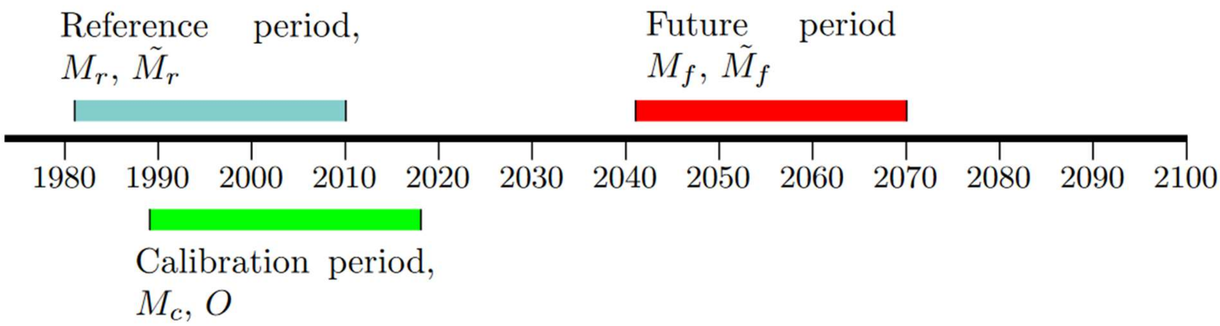

Figure 2. Different time periods used in this work, and nomenclature.

3.1.2. Methods

Calibration methods generally determine a mapping between model and observations from the calibration period. The mappings will be based on the distributional properties of the timeseries, but will be applied to the time-series themselves. However, the mappings used here are all monotonic, resulting in a series that preserves the main temporal characteristics of the model. This may be important to some users as the temporal characteristics of the model are not always realistic.

To this end we consider quantile-quantile mappings ('*q-q*' from now on). Let F_O and F_{Mc} be the cumulative distribution functions of observations and the corresponding model variable in the calibration period, respectively. Then $\Xi = F_O^{-1}(F_{Mc})$ is the mapping for the bias correction method and the calibrated values are $\tilde{M}_f = \Xi(M_f)$. Note that the distribution of $\Xi(M_c)$ is per definition identical to the distribution of O. For the δ-change the mapping is $\Xi = F_{M_f}^{-1}(F_{M_c})$ and the calibrated values $\tilde{M}_f = \Xi(O)$.

In particular for the *q-q* mappings there are in practice a number of choices that have to be made. These include the number of quantiles used to represent the cumulative distribution functions (if the lengths of the series are identical then number of quantiles can be the number of points in the series). Another important choice is the type of extrapolation used for values that fall outside the range of values in the calibration period (Figure 3). We force the extrapolation to pass through origin for variables wind (max and mean), shortwave radiation and evaporation. In Figure 3 we show the resulting inclinations for precipitation and temperature for RCP8.5. Evidently, RCP8.5 models are on average wetter (notably winters) and cooler (notably summers) than observations. No inclinations are extremely large, and we expect the method to be robust.

We must also decide if we want to work on daily or monthly values even if only monthly results are needed.

For the precipitation a particular problem arises regarding the treatment of wet days and dry days. After some testing we have chosen the following simple and robust method. We adjust model precipitation series to replicate the fraction of wet days in the calibration period.

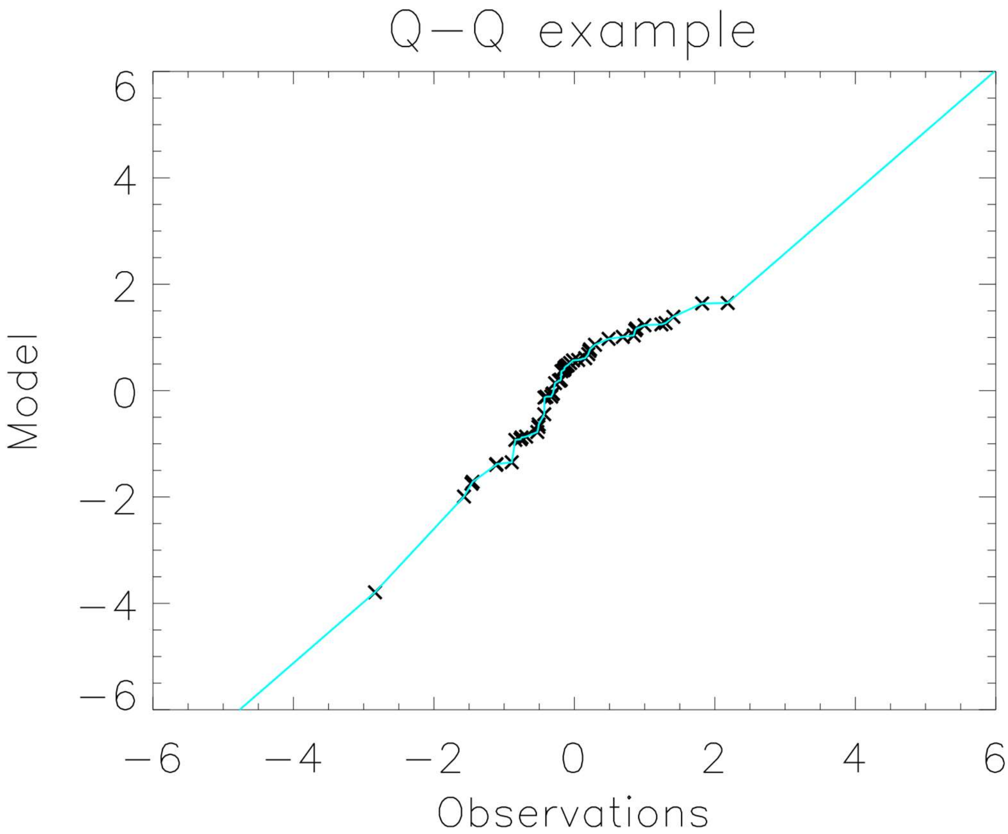

Figure 3 An example of how to extend the *q-q* map into the region without data. In this figure the last points to each side are extended with a straight line with the slope of the least squares line fitted robustly through all the points, which was our adopted method to deal with the ends of the distributions.

In the case where the model has more wet days than observation, the days with the lowest model precipitation will be converted to dry days. In the opposite case, we promote modelled dry days to wet days by promoting days with the highest sub-threshold precipitation to the threshold precipitation amount; if necessary, random dry days will be similarly promoted.

3.1.3. Summary

Details of cross-validation experiments examining the performance of bias-correction techniques can be found in previous versions of this report (e.g. DMI Report 24-11). In general, the following conclusions are drawn:

- In general, bias correction seems to be the best method.
- Bias correction should be performed on daily data even if only monthly means are wanted.

There are some other considerations:

- Results are sensitive to length of calibration period, but in *Klimaatlas* the impact is minor since 30-year periods of calibration data are available.
- Bias correction gives temporal correlations as in model, not as in observations.
- For δ-change, the length of the calibrated series is limited by the length of the observations.
- We emphasize that these conclusions hold only for the average over many realizations and the situation may be different for a particular 'truth'/model combination. The conclusions are probably somewhat on the optimistic side as they are based on model/model comparison and not on real observations.

3.1.4. Implementation details

The following generic procedure describes the implementation of quantile-quantile matching in *Klimaatlas* to produce calibrated climate variables.

- **Regridding of observational data to the CORDEX grid** For all model grid points with at least 50% land coverage the nearest KGDK grid-point is found, and this 'nearest neighbour' time series is used as the assigned observational data point for that model grid point. We use nearest neighbour method, rather than interpolation, to avoid any smoothing of data implicit in most interpolation methods. Distance is calculated in the straight line - no great-circle calculation is performed. We determine whether the model grid cell has at least 50% land by inspecting the same grid-cell in the model land-sea mask. To ensure that small islands are included, for which the land-sea mask may indicate less than 50%, we specifically assign ls-mask values above 50% so that the data at the island have appropriate weight. This was done for Anholt and Læsø.
- **Bias Adjustment.** For each model, and for each of the 4+1 seasons, the 99 separate percentiles are determined for the observed data and for the model by interpolation in the assembled values. A robust linear regression is then performed using the 99 data-pairs, and the slope of the regression line is noted. The slope is used to linearly extend the 99-point sequence beyond its range - to higher and lower values. See Figure 3 for an illustration of the procedure. The linear extensions are made starting in the last and first points of the sequence with the previously noted slope. On scenario data a quantile-quantile transformation is now performed using this constructed relationship. It is based on linear interpolation between points on the 99-pair percentile sequence if the interpoland (that is, the scenario value) is between the max and min of the sequence ordinate. If the interpoland falls either above or below the max and min of the ordinate range the linear extensions are used. The MATLAB robust regression routine is `robustfit`. When the 4 seasons have been completed, the results are combined to provide the annual time series.

3.1.5. Joint calibration of temperature maxima and minima

Daily maximum and minimum temperatures represent a special case, where there is a need to maintain the relative relationship between the two variables at once. For example, at no point in the time series should the daily minimum exceed the daily maximum. While multi-dimensional bias-correction methods could be considered, in *Klimaatlas* we have used a simpler approach by calibrating the daily temperature-range using the steps below.

- The modelled daily temperature range ($DTR = T_{max} - T_{min}$) was QQ-scaled against gridded observations for the period 2011-2019, resulting in DTR_{BA}. All instances where $DTR_{BA} < 0$ were set to 0.
- The skewness $Z = T_{mean} - (T_{max} + T_{min})/2$ was calculated for model data and then QQ-scaled against gridded observations, resulting in Z_{BA}.
- Then bias adjusted T_{min} and T_{max} were calculated using the equations $T_{min,BA} = T_{mean,BA} - Z_{BA} - DTR_{BA}/2$ and $T_{max,BA} = T_{mean,BA} - Z_{BA} + DTR_{BA}/2$.

The KGDK data for daily maximum and minmum temperatures used here is limited to the period 2011-2019. In 2011, a change in observing praxis occurs: before end of 2010 data were recorded from 6AM to next 6AM, but after start of 2011 it was recorded midnight to midnight.

While T_{max} is very likely always recorded at a cadence of one day, we suspect that T_{min} may be recorded with occasionally unpredictable offsets of one day in the older system of recording because the coldest time of day is usually in the morning hours - sometimes before 6 AM, sometimes after - thus producing the larger variation in Z before end of 2010. This problem effectively limits us to use data after the start of 2011 for indexes involving bias-adjusted temperature maxima and minima (Figure 4).

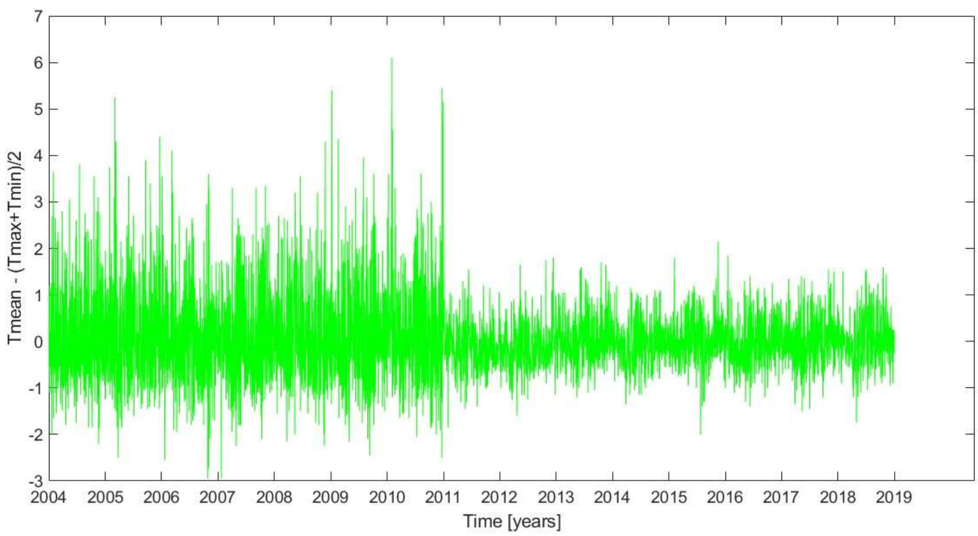

Figure 4 The skewness ($Z = T_{mean} - (T_{max} + T_{min})/2$) of 20x20 km gridded KGDK maximum and minimum temperature data changes at 2010/2011.

3.2. Quantile-quantile for precipitation

For the precipitation a particular problem arises regarding the treatment of wet days and dry days. After some testing we have chosen the following simple and robust method. We adjust model precipitation series to replicate the fraction of wet days in the calibration period. In the case where the model has more wet days than observation, the days with the lowest model precipitation will be converted to dry days. In the inverse case, we promote modelled dry days to wet days by promoting days with the highest sub-threshold precipitation to the threshold precipitation amount; if necessary, random dry days will be similarly promoted.

Two further modifications of the generic approach are also applied:

- Before application of the BA algorithm all zero values are set to a small random number between 0 and 10^{-12} in model and observations; after BA all adjusted model numbers smaller than 0.1 are set to zero.
- Extrapolation of the quantile-quantile plot in the negative direction is done with a line passing through (0,0) which helps avoid negative values where none ought to be possible.

3.3. Extreme values

Extreme events occur rarely and therefore the empirical quantile-quantile calibration technique described in Section 3 cannot be used, since the tail of the empirical cumulative distribution function (CDF) is poorly defined. Therefore, for extreme events, extreme value analysis is applied, where the empirical CDF is replaced by an analytically formulated cumulative distribution function, as described below.

A brief summary of work examining the performance of bias-correction techniques for extreme precipitation follows. Full details of this work can be found in the corresponding publication [Schmith et al., 2023].

3.3.1. Extreme value analysis

In extreme value analysis (EVA) one considers a time series of e.g. hourly values, and the aim is to estimate the frequency of occurrence of rare events, often expressed as the T-year return level, which is the level that on average is exceeded once every T years.

We use the peak-over-threshold (POT) method, where all peak values above a specified threshold x_0 and separated by a minimum time span are considered. It is assumed that peak occurrences are independent and Poisson-distributed with parameter λ, which is the average number of exceedances (events) per year. Alternatively, λ can be specified, in which case x_0 is a stochastic variable.

It can be shown that under very general conditions the distribution of the peak exceedances $x - x_0 > 0$ are distributed as a Generalised Pareto distribution (GPD) with cumulative distribution function given by:

$$F_{GPD}(x - x_0) = 1 - \left(1 - \xi \frac{x - x_o}{\sigma}\right)^{1/\xi}, x > x_o \qquad 3.1$$

The T-year return level is determined as the level exceeded on average once every T years, and therefore the following holds:

$$\lambda T[1 - F_{GPD}(X_T - X_O)] = 1 \quad 3.2$$

from which we get

$$x_T = F_{GPD}^{-1}\left(1 - \frac{1}{\lambda T}\right) + x_o \quad 3.3$$

There are several procedures available for estimating the parameters from data, the most important being: maximum likelihood (ML), method of moments (MOM) and probability weighted moments (PWM). Hosking and Wallis [1987] and Hosking et al. [1985] demonstrate that PWM in general yields reliable results with low variance for the number of samples in this study, whereas in particular ML can be problematic. Therefore we use PWM in the following. For more details see Coles [2001].

3.3.2. Analytical quantile matching

In Section 4.2 the theoretical framework was presented for estimating extreme value distributions and associated return levels. This can be applied to obtain future projected values and climate factors, defined as the ratio between a future and a present value, which will be presented below.

We make use of Equation 3 above, which is valid both for M_c and for O and for any return period T . If we apply this to O and M_c we obtain the expression

$$(1 =)\lambda_{M_c} T[1 - F_{GPD,M_c}(M_{c,T} - M_{c0})] = \lambda_O T[1 - F_{GPD,O}(O_T - O_0)] \quad 3.4$$

relating $M_{c,T}$ and O_T, and after some manipulation, we arrive at

$$O_T = F_{GPD,O}^{-1}\left\{1 - \frac{\lambda_{M_c}}{\lambda_O}\left[1 - F_{GPD,M_c}(M_{c,T} - M_{c0})\right]\right\} + O_0 \quad 3.5$$

Equation 3.5 defines a transformation from $M_{c,T}$ to O_T, which then in the calibration procedure is applied to $M_{f,T}$ to obtain $\tilde{M}_{f,T}$.

3.3.3. Implementation details

The following procedure is used for rare precipitation events, except cloudbursts (see Generic Procedure 3 for that)

- Re-creation of Spildevandskommiteens NRM model (see [Gregersen et al., 2014b]). This results in a 10x10 km grid (on 'det Danske Kvadratnet') of the λ-parameter (number of exceedances of the threshold per year) and the scale-parameter for a generalized Pareto distribution. Both for 1-hour data and 24-hour data.

- For the calibration-period and the reference as well as the three future periods, for land points only, for RCP4.5 and RCP8.5, we apply nearest-neighbour interpolation from the CORDEX model grid to the 10x10 km grid. The nearest-neighbour interpolation assigns the model series in the nearest CORDEX gridpoint to 'det Danske Kvadratnet' point under consideration.

- Perform extreme value analysis for all models and the calibration period and all scenarios, and 1 and 24-hour data. 24-hour analysis performed with sliding windows covering 24-hours but advancing one hour each step).
- For lower and lower thresholds find model points exceeding the threshold until $\lambda = 3$ (events/year) is found (this will be a different threshold for each model, period and landpoint, but all with $\lambda = 3$. Ensure at least 24 hours between each selected event.
- Fit a generalized Pareto distribution to the selected values, using the probability weighted method. Thereby find local scale and shape parameters.
- Average the shape parameter to one national value.
- Calculate return-levels from the GP parameters for the calibration-period.
- use the parameterized *q-q* transformation (see section 4) to correct the return-levels of the calibration period.
- In the reference-period and the three future periods correct the return-levels using the parameterized *q-q* transformation determined in the calibration period (with Equation 3.5).
- Files with *q-q* corrected return-values are prepared for the reference-period and the three future periods, for the next processing steps.

4. Sea level and storm surge indicators

In *Klimaatlas* we provide the projections of mean sea level change (index201), as well as for the changes in extreme sea levels until the end of the 21st century. They are calculated for the 36 coastal stretches defined by Kystdirektoratet (KDI), except Ringkøbing Fjord and Nissum Fjord, which are regulated by lock gates (Table 3, KDI code VK2 and VK3). Each coastal stretch is represented by one station (Table 5), chosen to have the most reliable present day high water statistics for the coastal stretch. The changes in extreme sea levels are represented by 1) changes in return levels (indices 202, 203, 204, 206, 208); and 2) changes in the frequencies of extreme sea level events (indices 210, 213). On our website we provide all projections for the start (2011-2040), mid- (2041-2070) and end-century (2071-2100) 30-year periods, for the very low (SSP1-1.9), low (SSP1-2.6), medium (SSP2-4.5), high (SSP3-7.0), and very high (SSP5-8.5) emission scenarios. Additionally, we provide a table with yearly projections for all scenarios. Sea level indicators are given as change compared to the 1995 baseline.

4.1. Data

The sea level indicators in *Klimaatlas* are based on the sea level projections data set (Garner et al., 2021) associated with the Intergovernmental Panel for Climate Change Sixth Assessment Report (IPCC AR6; Fox-Kemper et al., 2021). This data set was created using the Framework for Assessment of Changes To Sea-level (FACTS; Kopp et al., 2023) and contains the projections of the total sea level change, as well as for each of the contributions separately. The contributions are Antarctic and Greenland ice sheet, glaciers, land water storage, ocean dynamics (including thermal expansion of the ocean), and vertical land motion. All projections are given every 10 years from 2020 until the end of the 21st century or longer, as sea level change relative to the 1995-2014 reference period. The projections are given for every grid point on a regular 1°×1° grid and for all stations in the Permanent Service for Mean Sea Level database (PSMSL, 2024; Holgate et al., 2013).

There are two types of projections in the data set: 1) those based only on processes for whose projections we have medium or high confidence in, thus called medium confidence projections; and 2) those that additionally rely on processes for which we have only low confidence but if they happen could significantly increase sea level, such as the ice-shelf collapse and instability, which are therefore named low confidence projections. The medium confidence projections are given for five scenarios: SSP1-1.9, SSP1-2.6, SSP2-4.5, SSP3-7.0, and SSP5-8.5, and low confidence for three: SSP1-2.6, SSP2-4.5, and SSP5-8.5. When available, we choose to present the low confidence projections in *Klimaatlas* because, as noted in IPCC AR6, stakeholders with a low risk tolerance such as those planning for coastal safety, may wish to consider the estimates above the likely range, but we also provide a table with projections for all scenarios, with both low and medium confidence.

We also use the extreme sea level statistics provided by Kystdirektoratet (KDI). KDI provide a new set of return levels based on tide gauge records approximately every five years. The newest statistics were published in 2024 (Højvandsstatistikker, 2024) and contain return levels for 20, 50, 100, and 200-years return periods, including the uncertainties, determined from a generalized Pareto distribution based on 40 highest observed water levels at each station, from the beginning of the observations at that location until 01-01-2024. We also use an earlier version of their statistics (Højvandsstatistikker, 2012), which provides 1-year return levels obtained by directly counting the events in the tide gauge records.

Despite the IPCC dataset containing the vertical land motion (VLM) contribution, which mainly consists of the land uplift due to glacial isostatic adjustment (GIA), we instead use the VLM model from DTU Space (2015), which is also used in the KDI statistics (2024), to be consistent. Since the vertical land motion is an important contributor to sea level change in Denmark and it varies significantly across the country, this model, specifically made for Denmark, has a higher spatial resolution and thus covers local and regional differences better.

4.2. Sea level change

We extract the projections for individual sea level change contributions from the Greenland and Antarctic ice sheets, glaciers, land water storage, and ocean dynamics (incl. thermal expansion) for the 34 locations in *Klimaatlas* from the IPCC dataset. The IPCC dataset contains projections for both a regular 1° longitude-latitude grid, as well as for the locations of all stations in the Permanent Service for Mean Sea Level (PSMSL) database. We therefore apply two methods of extraction: 1) for locations that are in the PSMSL database and for locations that are very close to a grid point (less than 5 km), we use nearest neighbor interpolation and directly take the IPCC projection belonging to that location; 2) for the remaining locations we use bi-linear interpolation from the four closest grid points. We extract values for the 10th, 50th (median), and 90th percentile for years from 2020 to 2100.

The ocean dynamics contribution for the SSP2-4.5 (medium emission) climate scenario has extremely high values at a few grid points within Denmark, significantly higher than in the SSP5-8.5 (high emission) scenario, which is not realistic. Since the ocean dynamics contribution should not vary significantly across Denmark, to mitigate that we instead use the median of all grid points between 7°E and 16°E and 54°N and 58°N for every location for all scenarios.

We calculate the VLM contribution to sea level change from the same VLM model rates that were used to create the Højvandsstatistikker (2024), relative to the same reference period the IPCC dataset uses (1995-2014).

We then combine all sea level change contributions, both from the IPCC dataset and the separate VLM model. To get the total sea level change, we need to combine the contributions for both the median and the uncertainties:

$$SLR_{tot}^{50} = \sum_i SLR_i^{50} \tag{4.1}$$

$$\Delta SLR_{tot} = \sqrt{\sum_i (\Delta SLR_i)^2} \tag{4.2}$$

where SLR_{tot}^{50} is the median of the total sea level change, SLR_i^{50} median of each contribution *i*, ΔSLR_{tot} the uncertainty of the total and ΔSLR_i individual contribution uncertainties. The lower and upper uncertainties of some contributions, and therefore of the total sea level change, can be vastly different, so they are calculated separately as:

$$SLR_{tot}^{50} = \sum_i SLR_i^{50} \tag{4.3}$$

$$\Delta SLR^{10/90} = \left|SLR^{50} - SLR^{10/90}\right| \tag{4.4}$$

where $SLR^{10/90}$ are the 10th and the 90th percentiles of sea level change and $\Delta SLR^{10/90}$ are the lower and the upper uncertainty. With that, the equations used to calculate the 10th and the 90th percentile are:

$$SLR_{tot}^{10} = SLR_{tot}^{50} - \sqrt{\sum_i \left(SLR_i^{50} - SLR_i^{10}\right)^2} \quad 4.5$$

$$SLR_{tot}^{90} = SLR_{tot}^{50} + \sqrt{\sum_i \left(SLR_i^{50} - SLR_i^{90}\right)^2} \quad 4.6$$

Since the VLM model does not include uncertainties, we assume they are zero and use the same values as both median and 10th and 90th percentile.

The IPCC dataset provides projections with a 10 year temporal resolution starting from year 2020, as change relative to the 1995-2014 reference period. Since we need values from 2011 to be able to provide the average projection for the 2011-2040 period, we interpolate the sea level change between the reference period centered around year 2005, where the change is zero by definition, and the start of the projections. We also interpolate to yearly values for the whole time span for which we provide the projections. To provide projections relative to year 1995 (center of the 1981-2010 period), as in the previous versions of *Klimaatlas*, we shift all time series by assuming the change before the IPCC reference period is linear.

4.3. Return levels of extreme sea level events

We extract the 20, 50, and 100-year return levels from the most recent KDI statistics (2024), and the 1-year return level from the earlier KDI statistics (2012) for each of the 34 stations in *Klimaatlas*. Return levels from both datasets are adjusted to our 1995 reference using the rates given for each station in the KDI 2024 data set. We then interpolate between them in the log-period space to obtain the 5-year return level at each location.

The observations at the station Fåborg, representative for the Sydfynske Øhav coastal stretch, only started in 2000, so the observed time series was too short to be included into the KDI 2012 statistics. For the longer series, the 40 highest observed sea levels used to find the return level distribution are usually well above the 1- or even 5-year return periods, making it unsuitable to determine the 1-year return levels from it. However, since the Fåborg time series is so short, it has many data points with short return periods, so the fitted curve is reliable at low return periods. Therefore, for Fåborg we take the 1- and 5-year return levels from the KDI 2024 distribution.

To calculate future projections of extreme sea levels we combine the historical storm surge statistics with the sea level rise using again the same principles as in equations (1) and (4), which for return levels are:

$$RL_{proj}^{50} = RL_{hist}^{50} + SLR_{tot}^{50} \quad 4.7$$

$$RL_{proj}^{10} = RL_{proj}^{50} - \sqrt{\left(RL_{hist}^{50} - RL_{hist}^{10}\right)^2 + \left(SLR_{tot}^{50} - SLR_{tot}^{10}\right)^2} \quad 4.8$$

$$RL^{90}_{proj} = RL^{50}_{proj} + \sqrt{\left(RL^{50}_{hist} - RL^{90}_{hist}\right)^2 + \left(SLR^{50}_{tot} - SLR^{90}_{tot}\right)^2} \quad 4.9$$

where RL^{10}_{proj}, RL^{50}_{proj}, and RL^{90}_{proj} are the 10th, 50th, and 90th percentile of the projected future return levels, RL^{10}_{hist}, RL^{50}_{his} , and RL^{90}_{hist} represent the historical storm surge statistics, and SLR^{10}_{tot}, SLR^{50}_{tot}, and SLR^{90}_{tot} are the median and uncertainties of the total sea level change calculated above. We do this calculation for all the years between 2011 and 2100 and all scenarios provided in the IPCC database.

4.4. Frequency of extreme sea level events

We then calculate what will in the future be the frequency of the 20- and 100-year events in the present climate. We first convert the return periods to logarithmic scale, then for each of the levels, we interpolate the projected return level curve to obtain the future return period. If the future frequency of extreme event is less than 1 event per year (lowest value in the return level curve), we linearly extrapolate the curve using the 1- and 5-year return levels. The same process is applied to the median and the 10th percentile. However, this process can result in extremely large values for the 90th percentile and in some cases for the median. We therefore set a limit to 3 extreme events per year. We then convert the future return period to frequency of events in 20 years for the 20-year event, and 100 years for the 100-year event.

Finally, we calculate the averages for the start- (2011-2040), mid- (2041-2070), and end-century (2071-2100) period for all indicators and for all emission scenarios.

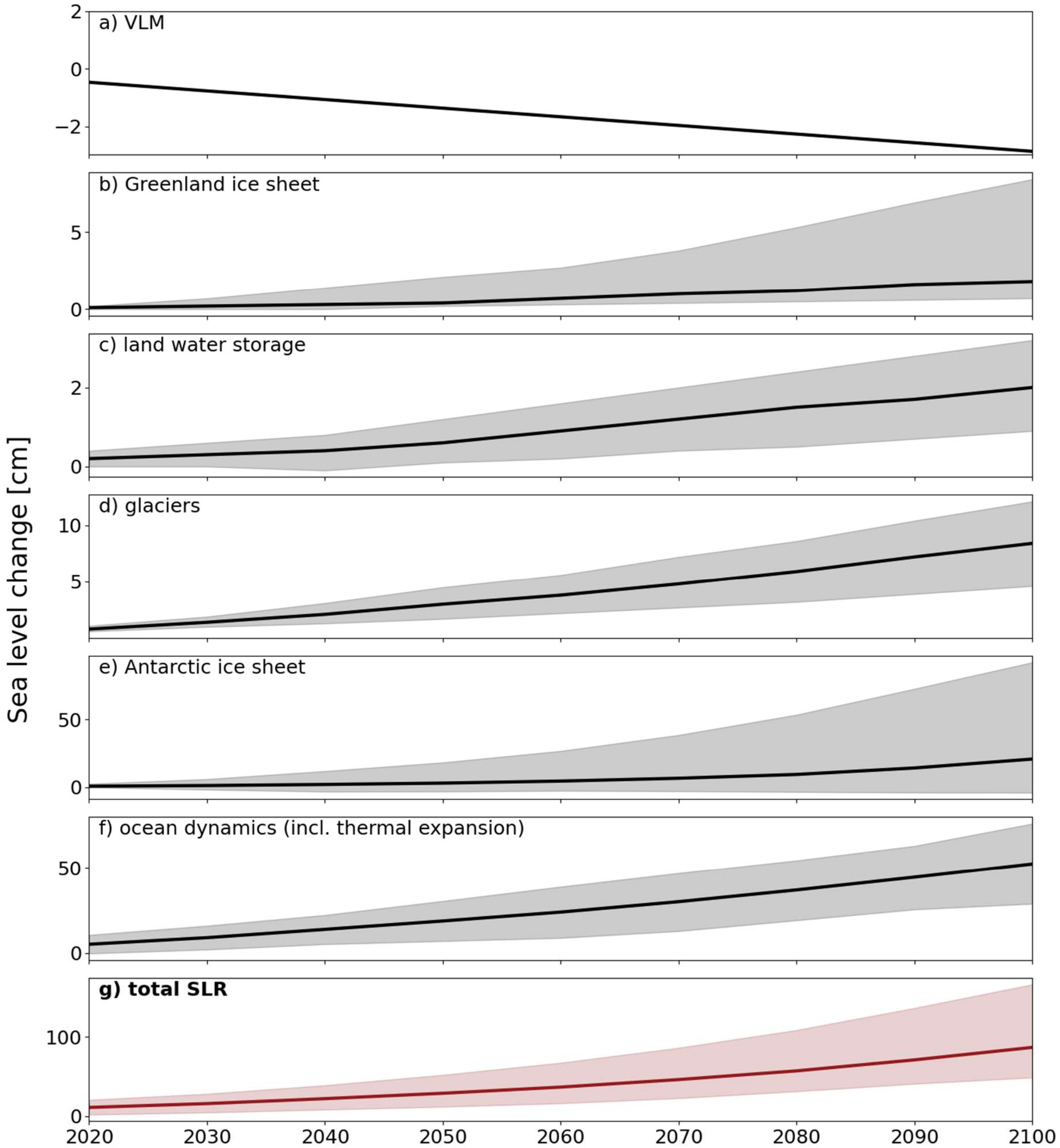

Figure 5 Sea level change contributions (a-f) and total sea level change (g) relative to the 1995-2014 reference period for the Vadehavskyst nordlig coastal stretch (represented by the station Esbjerg) in SSP5-8.5 scenario.

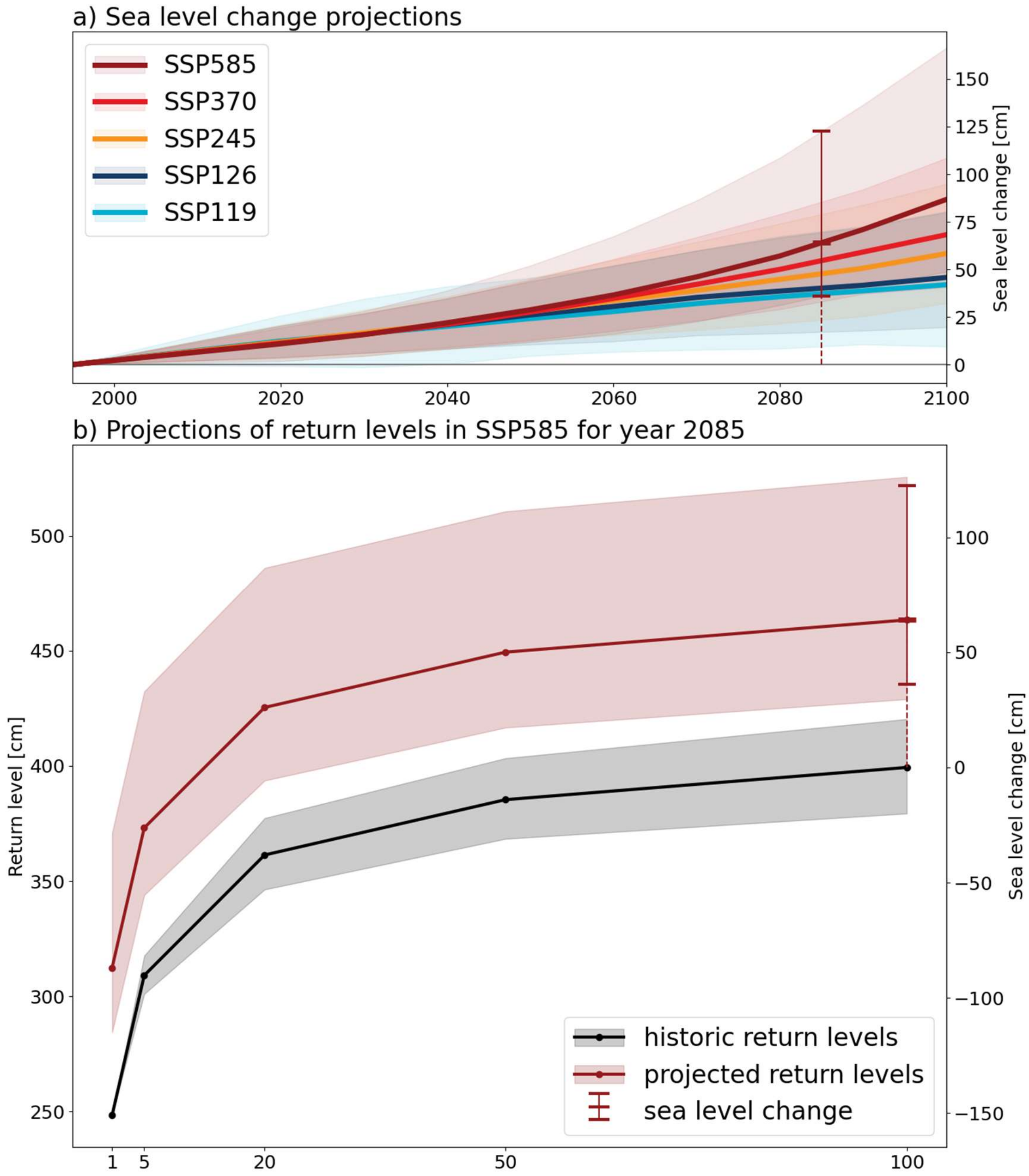

Figure 6 Calculating return levels for the Vadehavskyst nordlig coastal stretch (represented by the station Esbjerg) for year 2085 in the SSP5-8.5 scenario. (a) Projected sea level changes relative to the 1995-2014 reference period for the 5 SSP scenarios, with the blue vertical line showing the median and the uncertainties of the sea level change in year 2085 in SSP5-8.5. (b) Adding the sea level change to the historical return levels to obtain the return level projections in year 2085 in the SSP5-8.5 scenario.

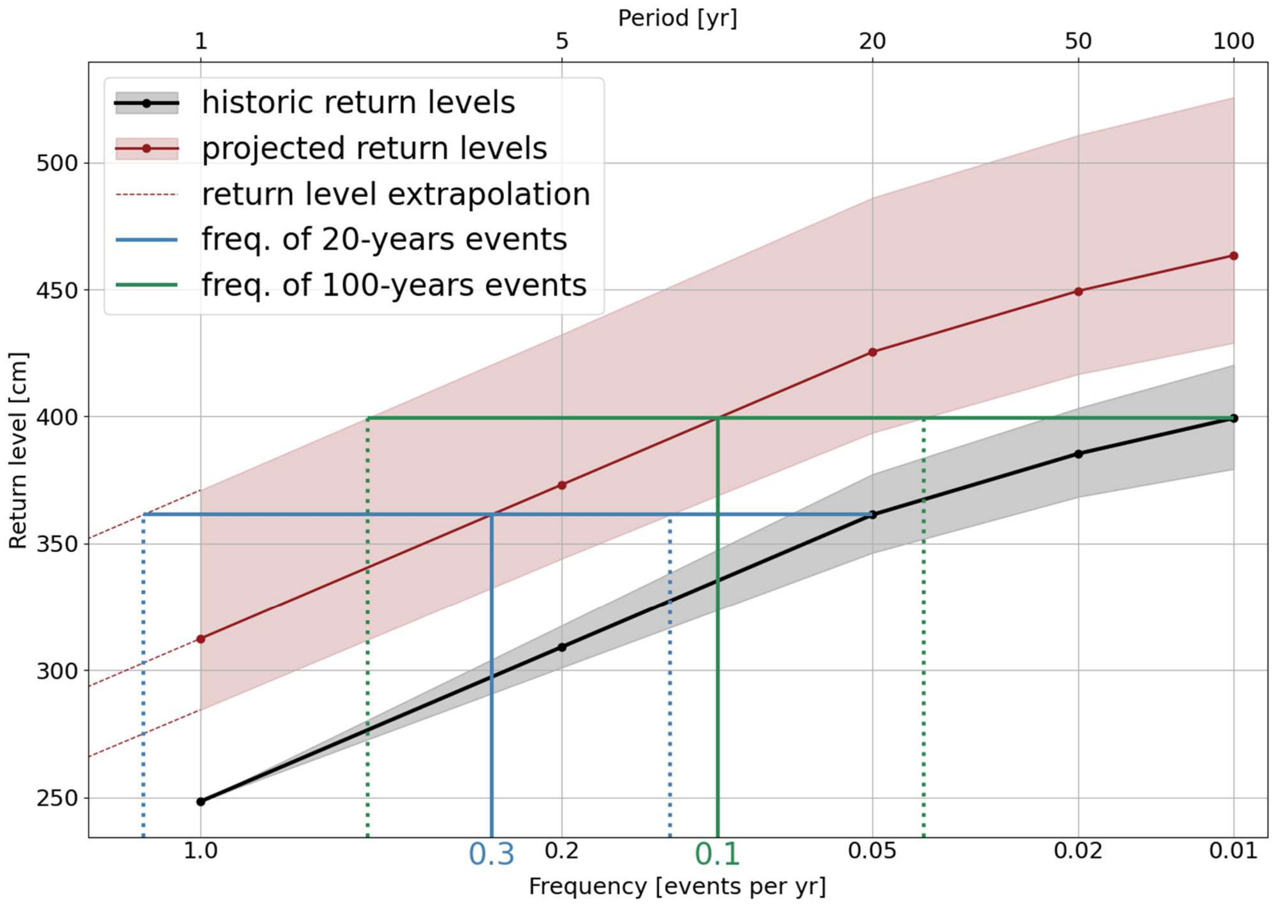

Figure 7 Calculating frequency indicators for the Vadehavskyst nordlig coastal stretch (represented by the station Esbjerg) for year 2085 in the SSP5-8.5 scenario.

Code	Coastal stretch	KDI ID	KDI Station	Longitude	Latitude	Warning Level (m)
VH1	Vadehavskyst syd	1	Vidå	8,65	54,96	2,40
VH2	Vadehavskyst central	6	Ribe	8,65	55,34	2,40
VH3	Vadehavskyst nord	7	Esbjerg	8,43	55,48	2,00
VK1	Vestkyst central	12	Hvide Sande Kyst	8,12	55,98	1,90
VK4	Vestkysten ud for Limfjorden	19	Thyborøn Kyst	8,21	56,73	1,90
VK5	Skagerrakkyst syd	20	Hanstholm	8,62	57,18	1,30
VK6	Skagerrakkyst nord	21	Hirtshals	9,96	57,63	1,30
LF1	Limford øst	31	Ålborg Øst	9,90	57,10	1,30
LF2	Limfjorden ved Skive	25	Skive	9,10	56,60	1,30
LF3	Limfjorden ved Lemvig	24	Lemvig	8,30	56,60	1,30
LF4	Limfjorden ved Thisted	27	Thisted	8,70	57,00	1,30
OJ1	Kattegatkyst nord	23	Frederikshavn	10,56	57,43	0,90
OJ2	Ålborg Bugt	33	Hals	10,46	56,96	1,30
OJ3	Randers Fjord og Mariager Fjord	34	Randers	10,26	56,58	1,25
OJ4	Djurslands østkyst og Anholt	35	Grenå	10,94	56,42	1,25
OJ5	Århus Bugt	36	Århus	10,21	56,14	1,25
OJ6	Lillebælt nord	38	Juelsminde	10,02	55,71	1,50
OJ7	Lillebælt central	40	Fredericia	9,75	55,56	0,84
SD1	Lillebælt syd	45	Fynshav	9,99	55,00	1,25
SD2	Sydfynske Øhav	46	Fåborg	10,23	55,10	1,00
SD3	Storebælt sydvest	51	Slipshavn	10,83	55,28	0,90
SD4	Femern Bælt	67	Gedser	11,92	54,57	1,25
SD5	Smålandsfarvandet	53	Karrebæksminde	11,65	55,17	0,95
SD6	Falsters og Møns Østersøkyst	66	Hesnæs	12,13	54,80	1,25
SD7	Faxe Bugt	64	Rødvig	12,38	55,25	1,25
SJ1	Storebælt nordvest og Odense Fjord	50	Kerteminde	10,67	55,45	1,00
SJ2	Storebælt nordøst	55	Kalundborg	11,09	55,67	1,10
SJ3	Sejrø Bugt	37	Ballen	10,65	55,82	1,25
SJ4	Nordsjællands kyst	60	Hornbæk	12,46	56,10	1,10
SJ5	Isefjord	57	Holbæk	11,70	55,73	1,00
SJ6	Roskilde Fjord	58	Roskilde	12,08	55,65	0,90
SJ7	Øresunds kyst	61	København	12,60	55,70	1,40
SJ8	Køge Bugt	63	Køge	12,20	55,45	1,10
SJ9	Bornholms kyst	69	Tejn	14,87	55,28	1,25

Table 3 Coastal stretches used in *Klimaatlas* together with details of the corresponding representative station from KDI's *Højvandstatistikker* (5. November 2024) and the corresponding local warning level.

5. Indicators

Climate indicators are the final output of *Klimaatlas* and can be generated via two different pathways. In the first pathway they are calculated based on one or more climate variables. However, climate indicators can also be calculated directly from inputs, as is seen in the case of sea level and storm surge indicators, and extreme precipitation statistics. This section provides an overview of all climate indicators in *Klimaatlas* and collates notes regarding the implementation of individual indices.

5.1. Overview

The current list of climate indicators in *Klimaatlas* is given in Table 4.

Indicator ID	Name	Description
001	Mean temperature	Mean temperature in °C over a year or a season.
002	Daily maximum temperature	The mean daily maximum temperature (in °C) seasonally or annually. Describes the highest temperature to be expected on a typical day.
003	Daily minimum temperature	The mean daily minimum temperature (°C) seasonally or annually. Describes the lowest temperature to be expected on a typical day.
004	Maximum temperature	The maximum temperature (°C) in the season/annually, calculated as the mean of the 30 years' occurrences seasonally/annually.
005	Minimum temperature	The minimum temperature (°C) in the season/annually, calculated as the mean of the 30 years' occurrences seasonally/annually.
006	Annual temperature range	Average annual difference between highest and lowest temperature in °C
007	Diurnal temperature range	Seasonal/annual average (in °C) of the range between daily maximum and minimum temperatures.
008	Heatwave days	Number of heat-wave days annually. A 'heatwave day' is indicated when the average of the maximum temperature, over at least three consecutive days, is above 28°C, not counting the first two days of each heatwave.
009	Warm-wave days	Number of warm-wave days annually. A 'warm-wave day' is indicated when the average of the maximum temperature, over at least three consecutive days, is above 25°C, not counting the first two days of each warm-wave.
010	Frost days	Number of days seasonally/annually where the lowest temperature is below freezing (0 °C).
011	Growing season length	Number of days between the years' first contiguous 6 days of daily mean temperature above 5 °C to the years last 6-day period of daily mean temperatures above 5 °C.
101	Mean precipitation	Mean precipitation in mm/day across a year or a season.
102	Max daily precipitation	Sum of precipitation during that day of the year or season when maximum 24-hour precipitation-sum was observed.
103	5-day max precipitation	5-day sum of precipitation in that 5 day period of the year or season with largest 5-day sum of precipitation.
104	14-day max precipitation	14-day sum of precipitation in that 14 day period of the year or season with largest 14-day sum of precipitation.

Indicator ID	Name	Description
105	Number of days with over 10 mm precipitation per day.	Number of days in a year/season with more than 10mm precipitation
106	Number of days with over 20 mm precipitation per day.	Number of days in a year/season with more than 10mm precipitation
107	Number of cloudbursts per year	Number of days with more than 15 mm precipitation in 30 minutes
108	Number of dry days	Number of days of the year or season with precipitation below 1 mm.
109	Maximum dry spell length	Length of the longest period of the year or season with consecutive days with precipitation below 1 mm.
110	Fraction of dry seasons	Proportion of "dry" years/ seasons, defined by total precipitation more than one standard deviation below the average for the historical period
112	Number of 5-day dry spells	Number of periods of minimum length 5 days with less than 1mm precipitation per day
115	Number of 10-day dry spells	Number of periods of minimum length 10 days with less than 1mm precipitation per day
151	2-year event hourly precipitation	Precipitation-sum for one hour that occurs with a return-period of two years.
152	5-year event hourly precipitation	Precipitation-sum for one hour that occurs with a return-period of five years.
153	10-year event hourly precipitation	Precipitation-sum for one hour that occurs with a return-period of ten years.
154	20-year event hourly precipitation	Precipitation-sum for one hour that occurs with a return-period of 20 years.
155	50-year event hourly precipitation	Precipitation-sum for one hour that occurs with a return-period of 50 years.
156	100-year event hourly precipitation	Precipitation-sum for one hour that occurs with a return-period of 100 years.
157	2-year event in 24-hour precipitation	Precipitation-sum over 24 hours that occurs with a return-period of two years.
158	5-year event 24-hour precipitation	Precipitation-sum over 24 hours that occurs with a return-period of five years.
159	10-year event 24-hour precipitation	Precipitation-sum over 24 hours that occurs with a return-period of 10 years.
160	20-year event 24-hour precipitation	Precipitation-sum over 24 hours that occurs with a return-period of 20 years.
161	50-year event 24-hour precipitation	Precipitation-sum over 24 hours that occurs with a return-period of 50 years.
162	100-year event 24-hour precipitation	Precipitation-sum over 24 hours that occurs with a return-period of 100 years.
201	Mean sea level	Mean sea-level with respect to coastline
202	Storm surge 20-year events	Height of storm surge, in cm, of the 20-year event, relative to reference level.

Indicator ID	Name	Description
203	Storm surge 50-year event	Height of storm surge, in cm, of the 50-year event, relative to reference level.
204	Storm surge 100-year event	Height of storm surge, in cm, of the 100-year event, relative to reference level.
206	1-year sea level event	Height of the sea level, in cm, of the 1 year event, relative to reference level.
208	5-year sea level event	Height of the sea level, in cm, of the 5 year event, relative to reference level.
210	Frequency of storm surge 20-year event	Frequency with which the historical 20-year storm surge level will be exceeded in a future climate
213	Frequency of storm surge 100-year event	Frequency with which the historical 100-year storm surge level will be exceeded in a future climate
301	Mean wind speed	Average wind speed (in m/s) over a year or a season.
302	Extreme wind	Number of days in a year or season with a maximum wind speed above 25 m/s.
401	Solar radiation	Seasonal/annual average of the daily sum of the direct and diffuse radiation from the Sun reaching the (horizontal) surface, in W/m2.
402	Potential evaporation	The seasonal/annual average potential evaporation (in mm/day) that could evaporate, as given by the Makkink formula Jacobs and Bruin [1998]
501	Mean Fire Weather Index	Mean FWI across seasons and year
502	Days with very high fire risk	Number of days with fire weather index above 18.5
503	Days with extremely high fire risk	Number of days with fire weather index above 29.5

Table 4. Indicators available in the current version of *Klimaatlas.*

5.2. Notes on individual indicators

This section lists notes regarding the implementation of individual indicators.

5.2.1. 107 Cloudbursts

The definition of a cloudburst is precipitation exceeding 15 mm in 30 minutes, but none of the CORDEX models have this temporal resolution represented in their output. Therefore an alternative approach has been chosen. In the DMI Technical Report 19-06 [Cappelen, 2019], station observations in high temporal resolution have been analysed for the period 2011-2018. In an average year, 87 stations out of 258 have measured at least one cloudburst. This roughly corresponds to one every 3 years for the given network of stations, ignoring any regional variation in the probability. The ’calibration period’ for cloudbursts is therefore 2011-2018.

With the assumption that the occurrence of cloudbursts is associated with extremes in hourly precipitation, which is readily available from models, we use hourly precipitation with a present-day return period of 3 years as a proxy for the occurrence of cloudbursts.

The change in 3-year return-level in hourly precipitation can be obtained from the parameters of POT fits to present-day and future extreme precipitation. From the present-day parameters, the three-year return level can be obtained for each point. This value is now entered into the corresponding CDF for the future period, and the return frequency of this value can be calculated. The uncertainty is calculated as the pointwise spread among models.

5.2.2. Wind speed indicators (301 and 302)

Due to of large gradients in wind speed inland from the coasts, the smoothing is reduced compared to other indices: a 25 x 25 km filter is applied instead of the general 75 x 75 km filter.

5.3. Production of climate indicators from climate variables

Here we detail the generic additional processing steps employed to come from bias-corrected variables to indicators.

5.3.1. Relationship between tasmin, tasmax and tas

Initial explorations in the development of *Klimaatlas* revealed that the model-fields for temperatures, their maxima and their minima – which are delivered from CORDEX as separate files generated by the individual contributors – did not all fulfill such basic requirements as $T_{min} < T_{mean} < T_{max}$. So before starting the bias adjustment procedure for modelled daily minimum and maximum temperature, we made corrections for each model, each day and each grid cell so that T_{min} is given the lowest value of T_{min}, T_{mean}, T_{max}, and T_{max} is given the highest value of the three variables and T_{mean} is given the middle value of the three.

5.3.2. Index calculation

For each year, and each of the 4+1 seasons, and for each CORDEX model grid-point, in each model we calculate the index in question using the bias-adjusted data. Split the results into the 30-year long reference and future scenario periods (some models only have 29 years of data in the last of the future periods, and some end in November of the last year). Take means over the 30 values in each period, at each grid-point, and for each season etc. Calculate changes in indices (differences or ratios, in %, as appropriate, and noted for each index below) between the future periods in question and the reference period.

5.3.3. Regrid indices to the KGDK 1x1 km grid.

Use the MATLAB routine `scatteredInterpolant` with option ’natural’. This ’smooths the result’ into neighbouring cells to a small degree. The 1x1 km land-sea mask is applied to remove apparent values over sea points.

Smooth the observed results with MATLAB routine `smooth2a` using square 25x25 km windows - the window moves in 1-km steps; smooth projections for the future with 75x75 km windows.

5.3.4. Ensemble averaging

For each 1x1 km grid-point collect the 68 model-index values relevant for the season and extract the 10, 50 and 90 percentiles, using the MATLAB routine named `prctile` (used with the implicit argument “exact”), which interpolates in the values presented to it. This grid is one end-product for the homepage.

5.3.5. Area-aggregation

For each municipality or main catchment area, identify the 1x1 km grid-points inside the boundary polygon - i.e. find all grid-points with centre-coordinate inside the given polygon. Calculate the mean of the 10, 50 and 90 percentile data generated above. This product is another product for the homepage.

5.4. Emissions scenarios

The following emissions scenarios are currently presented in *Klimaatlas*. The scenario naming follows that of the IPCC and attempts to form a linkage between the relative concentration pathways (RCPs) of IPCC AR5 and CMIP5, and the shared socioeconomic pathways (SSPs) of IPCC AR6 and CMIP6.

Scenario description	Atmospheric indexes	Oceanic indexes
Very high	RCP 8.5	SSP 5-8.5
High	-	SSP 3-7.0
Medium	RCP 4.5	SSP 2-4.5
Low	RCP 2.6	SSP 1-2.6
Very Low	-	SSP 1-1.9

Table 5. Emission scenarios used in *Klimaatlas*.

5.5. RCP4.5 error bars

The number of RCP4.5 models is about a factor of 2.5 less than for RCP8.5 and this leads to unfortunate effects due to small sample size and model inter-correlations (the few models present are somewhat dependent). The error bars for RCP4.5 results therefore show a tendency to vary a lot between future time periods, as well as, now and then, having unrealistically small widths. This prompts us to apply an adjustment scheme so that we can present estimated error bars for RCP4.5 results that are realistic. We ensure that

- The RCP4.5 error bars in near future and mid-century are adjusted so that the smaller one is scaled to the width of the larger one, and
- the end of century error bar is scaled so that it is never the smallest of the three error bars.

The scaling algorithm applies a factor on the error bars, when scaling is called for, which retains the ratio of the upper (50 to 90 percentile interval) error bar to that of the lower (10 to 50 percentile) error bar, while keeping the median value fixed.

A larger ensemble of models would remedy this problem from the root, but the EUROCORDEX ensemble of models is limited in scope for the RCP4.5 scenario.

5.6. Land areas - municipalities and main catchment areas

The detailed implementation of the calculation of each index is given in the following.

For each index calculations proceed as follows: Annual and seasonal mean (or also max/min, depending on the nature of the index) values are calculated at each EUR-11 gridpoint from daily-mean model values. This gives 30 annual values for each of the chosen reference (historical and scenario) periods we have chosen. The mean of the 30 values is then taken. Then differences between historical and future periods are calculated for indices requiring relative changes. Then re-gridding and smoothing is applied to relative changes and absolute values to attain a smooth 1x1 km grid. 10, 50 and 90 percentile values are determined from these values.

5.7. Shapefiles

The following shapefiles were used as the basis for spatial averaging

- The boundaries for municipalities (*kommuner*) are defined by Styrelsen for Dataforsyning og Effektivisering (SDFE) and as this product can be updated we state here that the information was downloaded in May of 2018. Future updates by SDFE are bound to be have very minor impacts and are typically incremental when, typically, water-bodies (streams) and beach-lines change. See SDFE [2019]. The shapefile can be downloaded from: https://www.dmi.dk/fileadmin/klimaatlas/municipalities.json

- The boundaries for main catchment areas (*vandopland*) are given by Miljøstyrelsen [MST, 2019] and can be downloaded from https://www.dmi.dk/fileadmin/klimaatlas/DK_hovedvandoplande_klimaatlas_UTM32N.json

- Coastal stretches (*kystrækninger*) can be downloaded from: https://www.dmi.dk/fileadmin/klimaatlas/DK_kystinddeling_klimaatlas_UTM32N.json

5.8. Grid transformations

Interpolation is performed linearly to render the index values onto a 1x1 km grid ('det Danske Kvadratnet') from the EUR-11 grid of the models. The interpolation uses Matlab routine `scatteredInterpolant` which uses a Voronoi triangulation of the scattered sample points to perform interpolation. Natural neighbour interpolation is used via the `natural` option [Sibson,1981]. Further implementation details for the `scatteredInterpolant` routine is given at Mathworks [2019].

5.9. Smoothing

Smoothing of the resulting 1x1 km grid is performed to avoid unrealistic details. We smooth all fields, after interpolation, by taking averages over moving box-windows of size 25×25 km. Since observed spatial structure is more credible than modelled future spatial structures in changes, we smooth the projections spatially with a bigger (75x75 km) filter, before calculating index changes (exception for winds, see Section 8.3).

Details on *det Danske KvadratNet* are available at Danmarks Statistik [2019].

For each index relative as well as absolute values of the expected values of the period mean quantities are calculated. For relative changes we use the historical reference period 1981-2010, and the future periods 2011-2040, 2041-2070 and 2071-2100. These future periods are also used when giving the absolute values. The 10, 50 and 90 percentiles are calculated from the differences between the mean values over reference vs. scenario periods for each available model. The percentiles thus illustrate model-spread.

6. Software

The atmospheric-data methods described above are shown in diagrammatic form in the flowchart in Figure 11. The data resulting from these procedures are stored.

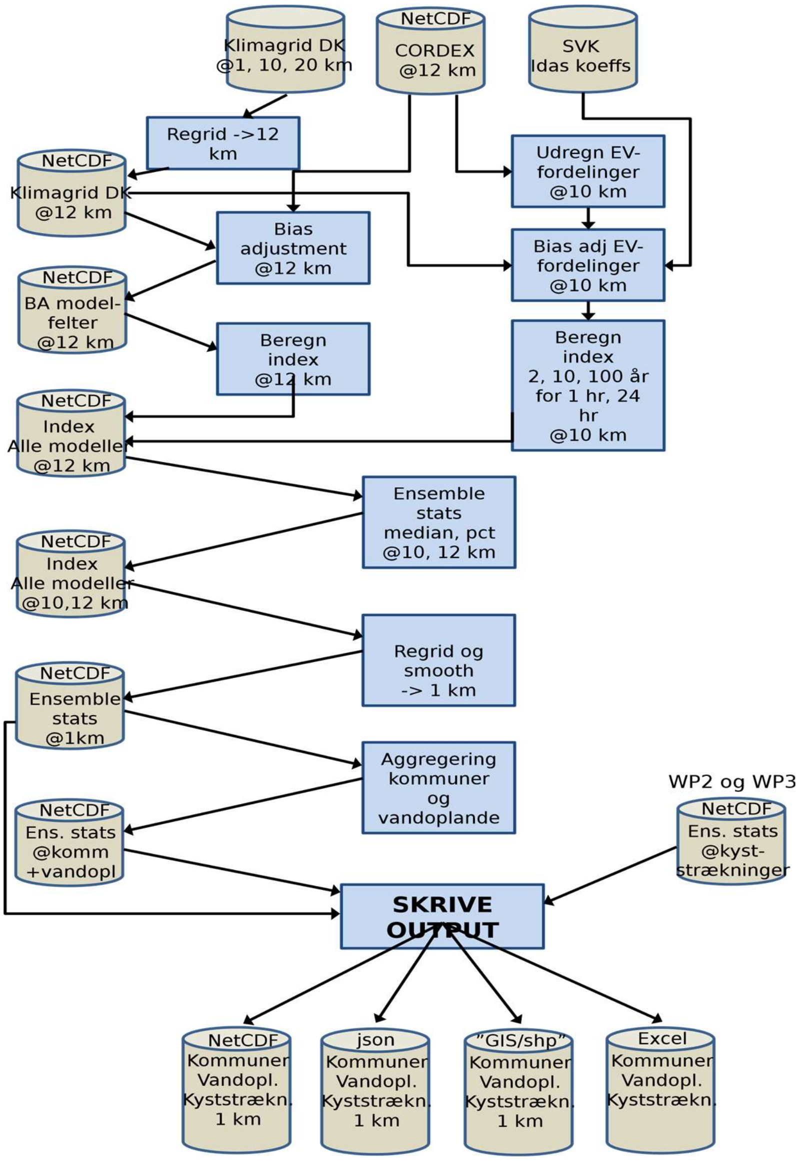

Figure 8. Flowchart showing the atmospheric-data processing steps.

7. Acknowledgements

We acknowledge the World Climate Research Programme’s Working Group on Regional Climate, and the Working Group on Coupled Modelling, former coordinating body of CORDEX and responsible panel for CMIP5. We also thank the climate modelling groups (listed in Table 1) for producing and making available their model output. We also acknowledge the Earth System Grid Federation infrastructure an international effort led by the U.S. Department of Energy’s Program for Climate Model Diagnosis and Intercomparison, the European Network for Earth System Modelling and other partners in the Global Organisation for Earth System Science Portals (GO-ESSP).” We thank the projection authors for developing and making the sea-level rise projections available, multiple funding agencies for supporting the development of the projections, and the NASA Sea Level Change Team for developing and hosting the IPCC AR6 Sea Level Projection Tool.

8. References

- Arns, T. Wahl, I.D. Haigh, J. Jensen, and C. Pattiaratchi. Estimating extreme water level probabilities: A comparison of the direct methods and recommendations for best practise. *Coastal Engineering*, 81:51–66, November 2013. doi: 10.1016/j.coastaleng.2013.07.003. URL https://doi.org/10.1016/j.coastaleng.2013.07.003.

- Jonathan L Bamber, Richard M Westaway, Ben Marzeion, and Bert Wouters. The land ice contribution to sea level during the satellite era. *Environmental Research Letters*, 13(6): 063008, jun 2018. ISSN 1748-9326. URL http://stacks.iop.org/1748-9326/13/i=6/a=063008?key=crossref.a29d19ff8e92d45a021c6aca08d2c874.

- Jonathan L. Bamber, Michael Oppenheimer, Robert E. Kopp, Willy P. Aspinall, and Roger M. Cooke. Ice sheet contributions to future sea-level rise from structured expert judgment. *Proceedings of the National Academy of Sciences*, 116(23):11195–11200, May 2019. doi:10.1073/pnas.1817205116. URL https://doi.org/10.1073/pnas.1817205116.

- Per Berg and Jacob Weismann Poulsen. Implementation details for hbm. Technical Report 12-11, Danish Meteorological Institute, 2012. URL https://www.dmi.dk/fileadmin/Rapporter/TR/tr12-11.pdf.

- John Cappelen. Ekstrem nedbør i danmark, opgørelser og analyser til og med 2016. Technical Report 17-06, Danish Meteorological Institute, 2017. URL https://www.dmi.dk/fileadmin/user_upload/Rapporter/TR/2017/DMIRep17-06.pdf.

- John Cappelen. Ekstrem nedbør i danmark - opgørelser og analyser til og med 2018, tr19-06. Technical report, Danish Meteorological Institute, 2019. URL https://www.dmi.dk/fileadmin/user_upload/Rapporter/TR/2019/DMIRap19-06.pdf.

- Bo Christiansen. Comparing cmip6 and cmip5: The road forward for the danish klimaatlas. Technical Report 22-38, Danish Meteorological Institute, 2022. URL https://www.dmi.dk/fileadmin/Rapporter/2022/DMI_rapport_22-38.pdf.

- Church, P. U. Clark, A. Cazenave, J. M. Gregory, S. Jevrejeva, A. Levermann, M. A. Merrifield, G. A. Milne, R. S. Nerem, P. D. Nunn, A. J. Payne, W. T. Pfeffer, D. Stammer, and S. Unnikrishnan. Sea-level rise by 2100. *Science*, 342(6165):1445–1445, December 2013a. doi: 10.1126/science.342.6165.1445-a.

- J.A. Church, P.U. Clark, A. Cazenave, J.M. Gregory, S. Jevrejeva, A. Levermann, M.A. Merrifield,G.A. Milne, R.S. Nerem, P.D. Nunn, A.J. Payne, W.T. Pfeffer, D. Stammer, and A.S. Unnikrishnan. *Sea Level Change*, book section 13, page 1137–1216. Cambridge University Press, Cambridge, United Kingdom and New York, NY, USA, 2013b. ISBN 978-1-107-66182-0.doi: 10.1017/CBO9781107415324.026 *Editors: Stocker, T.F. and Qin, D. and Plattner, G.-K. and Tignor, M. and Allen, S.K. and Boschung, J. and Nauels,and Xia, Y. and Bex, V. and Midgley, P.M.*

- Stuart Coles. *An Introduction to Statistical Modeling of Extreme Values*. Springer London, 2001. doi: https://doi.org/10.1007/978-1-4471-3675-0.

- Sönke Dangendorf, Marta Marcos, Guy Wöppelmann, Clinton P. Conrad, Thomas Frederikse, and Riccardo Riva. Reassessment of 20th century global mean sea level rise. *Proceedings of the National Academy of Sciences*, 114(23):5946–5951, May 2017. doi:10.1073/pnas.1616007114.
- Danmarks Statistik. Kvadratnet, 2019. URL https://www.dst.dk/da/TilSalg/produkter/geodata/kvadratnet.
- Robert M. DeConto and David Pollard. Contribution of antarctica to past and future sea-level rise. *Nature*, 531(7596):591–597, March 2016. doi: 10.1038/nature17145. URL https://doi.org/10.1038/nature17145.
- Charlotte Ditlevsen, Marta Ramos, Carlo Sørensen, Ulf Ciocan, and Thorsten Piontkowitz. Højvandsstatistikker 2017. Technical report, Kystdirektoratet, 2019. URL https://kyst.dk/media/80372/hoejvandsstatistikker2017revideret11022019.pdf.
- M. G. Donat, G. C. Leckebusch, S. Wild, and U. Ulbrich. Future changes in european winter storm losses and extreme wind speeds inferred from GCM and RCM multi-model simulations. *Natural Hazards and Earth System Science*, 11(5):1351–1370, May 2011. doi:10.5194/nhess-11-1351-2011. URL https://doi.org/10.5194/nhess-11-1351-2011.
- Markus G Donat, Gregor C Leckebusch, Simon Wild, and Uwe Ulbrich. Benefits and limitations of regional multi-model ensembles for storm loss estimations. *Climate Research*, 44(2-3):211–225, 2010. doi: 10.3354/cr00891. URL https://doi.org/10.3354/cr00891.
- T Edwards, L Brandon, M A G Durand, and N R Edwards. Revisiting antarctic ice loss due to marine ice-cliff instability. *Nature*, 566(7742):58–64, 2019. doi: doi:10.1038/s41586-019-0901-4. URL https://doi.org/10.1038/s41586-019-0901-4.
- Fox-Kemper, H.T. Hewitt, C. Xiao, G. Aðalgeirsdóttir, S.S. Drijfhout, T.L. Edwards, N.R. Golledge, M. Hemer, R.E. Kopp, G. Krinner, A. Mix, D. Notz, S. Nowicki, I.S. Nurhati, L. Ruiz, J.-B. Sallée, A.B.A. Slangen, and Y. Yu. Ocean, Cryosphere and Sea Level Change. In V. Masson-Delmotte, P. Zhai, A. Pirani, S. L. Connors, C. Péan, S. Berger, N. Caud, Y. Chen, L. Goldfarb, M. I. Gomis, M. Huang, K. Leitzell, E. Lonnoy, J. B. R. Matthews, T. K. Maycock, T. Waterfield, O. Yelekçi, R. Yu, and B. Zhou, editors, *Climate Change 2021: The Physical Science Basis. Contribution of Working Group I to the Sixth Assessment Report of the Intergovernmental Panel on Climate Change*, book section 4. Cambridge University Press, Cambridge, United Kingdom and New York, NY, USA, 2021, https://doi.org/10.1017/9781009157896.011
- W Fu, J She, and M Dobrynin. A 20-year reanalysis experiment in the Baltic Sea using three-dimensional variational (3DVAR) method. *Ocean Science*, 8(5):827–844, 2012. doi:10.5194/os-8-827-2012.
- Garner, G. G., T. Hermans, R. E. Kopp, A. B. A. Slangen, T. L. Edwards, A. Levermann, S. Nowikci, M. D. Palmer, C. Smith, B. Fox-Kemper, H. T. Hewitt, C. Xiao, G. Aðalgeirsdóttir, S. S. Drijfhout, T. L. Edwards, N. R. Golledge, M. Hemer, G. Krinner, A. Mix, D. Notz, S. Nowicki, I. S. Nurhati, L. Ruiz, J-B. Sallée, Y. Yu, L. Hua, T. Palmer, B. Pearson, 2021. IPCC AR6 Sea Level Projections. Version 20210809. Dataset accessed [2023-10-09] at https://doi.org/10.5281/zenodo.5914709.
- Gregory G Garner and Robert E Kopp. Framework for assessing changes to sea-level (FACTS) modules, scripts, and data for the IPCC AR6 sea level projections, 2022.

- B. Gregersen, H. Madsen, J.J. Linde, Krüger, and K. Arnbjerg-Nielsen. Opdaterede klimafaktorer og dimensionsgivende regnintensiteter Skrift nr. 30. Technical report, Spildevandskomiteen, 2014a.
- B. Gregersen, M. Sunyer, H. Madsen, S. Funder, J. Luchner, and D. Ros. Past, present, and future variations of extreme precipitation in denmark. Technical report, Danish Technical University, 2014b.
- Lonny Hansen. Sea level data 1889-2017 from 14 stations in denmark mean, maximum and minimum values calculated on monthly and yearly basis including plots of mean values. Technical Report 18-16, Danish Meteorological Institute, 2018. URL https://www.dmi.dk/fileadmin/Rapporter/2018/DMI_Report_18-16.pdf.
- Carling C Hay, Eric Morrow, Robert E Kopp, and Jerry X Mitrovica. Probabilistic reanalysis of twentieth-century sea-level rise. *Nature*, 517(7535):481, 2015. doi: doi:10.1038/nature14093.
- Simon J. Holgate, Andrew Matthews, Philip L. Woodworth, Lesley J. Rickards, Mark E. Tamisiea, Elizabeth Bradshaw, Peter R. Foden, Kathleen M. Gordon, Svetlana Jevrejeva, and Jeff Pugh. New data systems and products at the permanent service for mean sea level. *Journal of Coastal Research*, pages 493–504, 2013. doi: 10.2112/JCOASTRES-D-12-00175.1. URL https://doi.org/10.2112/JCOASTRES-D-12-00175.1.
- R. M. Hosking, J. R. Wallis, and E. F. Wood. Estimation of the Generalized Extreme-Value Distribution by the Method of Probability-Weighted Moments. *Technometrics*, 27(3):251, August 1985. ISSN 00401706. URL http://www.jstor.org/stable/1269706?origin=crossref.
- R.M. Hosking and J. R. Wallis. Parameter and quantile estimation for the generalized pareto distribution. *Technometrics*, 29(3):339–349, August 1987. URL https://doi.org/10.1080/00401706.1987.10488243.
- Daniela Jacob, Juliane Petersen, Bastian Eggert, Antoinette Alias, Ole Bøssing Christensen, Laurens M. Bouwer, Alain Braun, Augustin Colette, Michel Déqué, Goran Georgievski, Elena Georgopoulou, Andreas Gobiet, Laurent Menut, Grigory Nikulin, Andreas Haensler, Nils Hempelmann, Colin Jones, Klaus Keuler, Sari Kovats, Nico Kröner, Sven Kotlarski, Arne Kriegsmann, Eric Martin, Erik van Meijgaard, Christopher Moseley, Susanne Pfeifer, Swantje Preuschmann, Christine Radermacher, Kai Radtke, Diana Rechid, Mark Rounsevell, Patrick Samuelsson, Samuel Somot, Jean Francois Soussana, Claas Teichmann, Riccardo Valentini, Robert Vautard, Björn Weber, and Pascal Yiou. EURO-CORDEX: New high-resolution climate change projections for European impact research. *Regional Environmental Change*, 14(2):563–578, 2014. doi: 10.1007/s10113-013-0499-2.
- F G Jacobs and H. A R De Bruin. Makkink's equation for evapotranspiration applied to unstressed maize. *Hydrological Processes*, 12:1063–1066, 1998. ISSN 08856087. doi: 10.1002/(SICI)1099-1085(19980615)12:7<1063::AID-HYP640>3.0.CO;2-2.
- Thomas Jacobsen, Carlo Sørensen, Jacob Woge Nielsen, and Jian Su. Dmi report 21-28, historical extreme high water levels along the coastline of denmark final scientific report of the 2020 national centre for climate research work package 2.2.3 ekstremhav. Technical Report 21-28, Danish Meteorological Institute, 2021. URL https://www.dmi.dk/fileadmin/Rapporter/2021/DMI_Report_21-28.pdf.
- Kopp, R. E., Garner, G. G., Hermans, T. H. J., Jha, S., Kumar, P., Reedy, A., Slangen, A. B. A., Turilli, M., Edwards, T. L., Gregory, J. M., Koubbe, G., Levermann, A., Merzky, A., Nowicki, S., Palmer, M. D., &

Smith, C., 2023. The Framework for Assessing Changes To Sea-Level (FACTS) v1.0: A platform for characterizing parametric and structural uncertainty in future global, relative, and extreme sea-level change. Geoscientific Model Development, 16, 7461–7489. https://doi.org/10.5194/gmd-16-7461-2023

- Kystdirektoratet (KDI), Højvandsstatistiker 2012, https://kyst.dk/media/nibjjwhw/hoejvandsstatistikker_2012_rev_15072013.pdf

- Kystdirektoratet (KDI), Højvandsstatistiker 2024, https://kyst.dk/media/1ftbul3g/hoejvandsstatistikker-2024.pdf

- H. Madsen, I. B. Gregersen, D. Rosbjerg, and K. Arnbjerg-Nielsen. Regional frequency analysis of short duration rainfall extremes using gridded daily rainfall data as co-variate. *Water Science and Technology*, 75(8):1971–1981, February 2017. URL https://doi.org/10.2166/wst.2017.089.

- Moritz Mathis, B Mayer, and Thomas Pohlmann. An uncoupled dynamical downscaling for the North Sea: method and evaluation. *Ocean Modelling*, 72:153–166, 2013. URL https://doi.org/10.1016/j.ocemod.2013.09.004.

- Mathworks. The *scatteredInterpolant* routine, 2019. URL https://se.mathworks.com/help/matlab/ref/scatteredinterpolant.html.

- Jerry X Mitrovica and Glenn A Milne. On post-glacial sea level: I. General theory. *Geophysical Journal International*, 154(2):253–267, 2003. URL https://doi.org/10.1046/j.1365-246X.2003.01942.x.

- Jerry X Mitrovica, Natalya Gomez, and Peter U Clark. The sea-level fingerprint of West Antarctic collapse. *Science*, 323(5915):753–753, 2009. URL https://science.sciencemag.org/content/323/5915/753.

- Jerry X Mitrovica, N Gomez, E Morrow, C Hay, K Latychev, and ME Tamisiea. On the robustness of predictions of sea level fingerprints. *Geophysical Journal International*, 187 (2):729–742, 2011. URL https://doi.org/10.1111/j.1365-246X.2011.05090.x.

- MST. Miljøstyrelsen, 2019. URL https://mst.dk.

- Sanne Muis, Martin Verlaan, Hessel C Winsemius, Jeroen CJH Aerts, and Philip J Ward. A global reanalysis of storm surges and extreme sea levels. *Nature communications*, 7:11969, 2016. URL https://doi.org/10.1038/ncomms11969.

- Robert S Nerem, Brian D Beckley, John T Fasullo, Benjamin D Hamlington, Dallas Masters, and Gary T Mitchum. Climate-change–driven accelerated sea-level rise detected in the altimeter era. *Proceedings of the National Academy of Sciences*, 115(9):2022–2025, 2018. URL https://doi.org/10.1073/pnas.1717312115.

- Martin Olesen, Kristine Skovgaard Madsen, Carsten Ankjær Ludwigsen, Fredrik Boberg, Tina Christensen, John Cappelen, Ole Bøssing Christensen, Katrine Krogh Andersen, and

- Jens Hesselbjerg Christensen. Fremtidige klimaforandringer i danmark. Technical Report 14-06, DMI, 2014. URL https://www.dmi.dk/fileadmin/user_upload/Rapporter/DKC/2014/Klimaforandringer_dmi.pdf.

- Oppenheimer, Glavovic B., Hinkel J., R. van de Wal, A. Magen, A. Abd-Elgawad, R.S. Cai, Cifuentes-Jara, R.M. Deconto, T. Ghosh, J. Hay, F. Isla, B. Marzeion, B. Meyssignac, and Z. Sebesvari. *Sea Level Rise and Implications for Low Lying Islands, Coasts and Communities*, book 4. in press, 2019. URL www.ipcc.ch/srocc/download-report. Please be aware that this citation is the draft version, the final version will be available on the website after correction.

- Permanent Service for Mean Sea Level (PSMSL), 2024, "Tide Gauge Data", http://www.psmsl.org/.

- David T Pugh. *Tides, surges and mean sea level*. John Wiley and Sons Inc., New York, NY, 1987.

- Madleine Samuelsson and Anders Stigebrandt. Main characteristics of the long-term sea level variability in the baltic sea. *Tellus A*, 48(5):672–683, 1996. doi:10.1034/j.1600-0870.1996.t01-4-00006.x. URL https://onlinelibrary.wiley.com/doi/abs/10.1034/j.1600-0870.1996.t01-4-00006.x.

- Mikael Scharling. Klimagrid - danmark nedbør, lufttemperatur og potentiel fordampning 20x20 & 40x40 km - metodebeskrivelse. Technical Report 99-12, Danish Meteorological Institute, 1999. URL https://www.dmi.dk/fileadmin/user_upload/Rapporter/TR/1999/tr99-12.pdf.

- Mikael Scharling. Klimagrid Danmark nedbør 10x10 km (ver.2) - metodebeskrivelse. Technical Report 99-15, Danish Meteorological Institute, 2012. URL https://www.dmi.dk/fileadmin/user_upload/Rapporter/TR/1999/tr99-15.pdf.

- Torben Schmith, Peter Thejll, Flemming Vejen, and Bo Christiansen. Regional variation of climatological cloudburst frequency estimated from historical observations of daily precipitation sums. *International Journal of Climatology*, 11 2023. ISSN 0899-8418. doi:10.1002/joc.8291.

- SDFE. Styrelsen for dataforsyning og effektivisering, 2019. URL https://sdfe.dk/hent-data/datafordeleren/.

- R Sibson. A brief description of natural neighbor interpolation. In V Barnett, editor, *Interpreting multivariate data*, pages 21–36. Wiley, Chichester, 1981.

- Aimée BA Slangen, Benoit Meyssignac, Cecile Agosta, Nicolas Champollion, John A Church, Xavier Fettweis, Stefan RM Ligtenberg, Ben Marzeion, Angelique Melet, Matthew D Palmer, et al. Evaluating model simulations of twentieth-century sea level rise. Part I: global mean sea level change. *Journal of Climate*, 30(21):8539–8563, 2017. URL https://doi.org/10.1175/JCLI-D-17-0110.1.

- Carlo Sørensen, H.T. Madsen, and S.B. Knudsen. Højvandsstatistikker 2012. Technical report, Kystdirektoratet, 2013.

- Peter Riddersholm Wang and Mikael Scharling. Klimagrid danmark - dokumentation og validering af klimagrid danmark i 1x1 km opløsning. Technical Report 10-13, Danish Meteorological Institute, 2012. URL https://www.dmi.dk/fileadmin/Rapporter/TR/tr10-13.pdf.

- Y Wang, K R Anderson, and R M Suddaby. Updated source code for calculating fire danger indices in the canadian forest fire weather index system. information report nor-x-424, 2015. ISSN 0831-8247.

- Christopher S Watson, Neil J White, John A Church, Matt A King, Reed J Burgette, and Benoit

- Legresy. Unabated global mean sea-level rise over the satellite altimeter era. *Nature Climate Change*, 5(6):565–568, 2015. URL https://www.nature.com/articles/nclimate2635.

- Philip L Woodworth, JR Hunter, Marta Marcos, P Caldwell, Margarita Menéndez, and I Haigh. Towards a global higher-frequency sea level dataset. *Geoscience Data Journal*, 3(2):50–59, 2016. URL https://doi.org/10.1002/gdj3.42.

9. Appendix A Previous versions

Release notes describing previous versions of *Klimaatlas* can be found in this section. Data associated with each version is also found in the version archive on the webpage (https://www.dmi.dk/klima-atlas/versionshistorik) and in Zenodo archive (https://zenodo.org/communities/klimaatlas/).

9.1. Version v2024a, June 2024

This version introduces a new indicators related to fire, dry periods and meteorological drought. In addition, several existing precipitation indicators have been moved into a new "tørke" (drought) group. The new groupings and indicators (with their corresponding IDs) are:

- Fire danger (*brandfare*)
  - Average fire danger across years / seasons
  - Number of days with "very high" fire danger
  - Number of days with "extreme" fire danger
- Drought (tørke)
  - Number of dry days (moved from *Nedbør* (precipitation) group) (108)
  - Longest dry period (moved from *Nedbør* (precipitation) group) (109)
  - Number of years / season that are "dry" (110)
  - Number of periods of minimum five consecutive dry days (112)
  - Number of periods of minimum ten consecutive dry days

The number of ensemble members has been expanded from 65 to 72.

Klimaatlas data is now archived in the Zenodo archive. As a result, *Klimaatlas* data and reports now have a Digital Object Identifier (DOI) associated with them. This version of *Klimaatlas* can therefore be referenced as:

Danish Meteorological Institute. (2024). DMI Klimaatlas v2024a - Projections of climate indicators over Denmark [Data set]. Zenodo. https://doi.org/10.5281/zenodo.11402836

Previous versions of *Klimaatlas* data have also be archived retrospectively. The full archive can be found at: https://zenodo.org/communities/klimaatlas

Excel spreadsheets have been converted to a new format that is intended to be both human-readable and machine readable. The medium emissions scenario (RCP4,5 / SSP2-4,5) were added to the Kommune reports, together with overview "cartoon-strips" showing changes under different emissions scenarios.

9.2. Version v2022a, February 2023.

In this update of *Klimaatlas*, we added (1) the low emission climate scenario RCP2.6, (2) sea level projections from the latest IPCC report, and (3) additional climate model data for the RCP4.5 and RCP8.5 scenarios.

Regarding (1) and (3), the list of models used in the current data set can be found in Tables 7 and 8.

Regarding (2), we updated the mean sea level data regionalized from IPCC AR6, which means it is now based on the new generation of emission scenarios, “Shared Socioeconomic Pathways” (SSPs). The scenarios used in this report for sea level rise assessment are SSP12.6/RCP2.6, SSP2-4.5/RCP4.5 and SSP5-8.5/RCP8.5. As something new, our uncertainty estimates now include the expert judgement of potential contributions from melting ice sheets not well-captured by the climate models; often called low confidence processes, as part of "deep uncertainty" related to sea level rise. The inclusion of this estimate from the latest IPCC report results in a larger uncertainty interval, especially through an increased 90-percentile of the high-emission scenario RCP8.5.

Improved calculation methods have given rise to minor changes with this update. Among the atmospheric indices, we change the order of statistical processing and interpolation for some of the indices, with only small changes discernible in the mean. We have added an updated flow-chart of the processing used for the atlas, on page 30. Looking at the change in median values expressed as a percentage of the width of the old confidence interval from the 10 to the 90 percentile, we note some changes, mainly of minor sizes. Indices of wind and extreme precipitation show the most pronounced local changes.

With the method update, it appears that the older versions of *Klimaatlas* underestimated the widths of confidence intervals for indexes related to extremes, compared to the present version of *Klimaatlas*. Hence, these have increased - again - especially for extreme precipitation and winds.

Lastly, while the regional climate model projections of the SSP-scenarios are still being prepared by the international research community, we have added a first assessment of the new generation of global climate model projections (CMIP6, based on the SSP-scenarios) over Northern Europe and how they compare to the previous projections (CMIP5, based on RCP-scenarios). The assessment can be found in subsection (Section 5.1.1), with more details in the report Christiansen [2022].

9.3. Version v2021a, December 2021.

In this version we release high resolution time series for 8 variables, namely - tas, tasmin, tasmax, pr, sfcWind, sfcWindmax, rsds, potevap, which are used to produce a range of indexes in *Klimaatlas*. These time-series are released at a 1x1 km grid as daily values, and are made available as netcdf files for download by the users.

Users of these expert-only data should be aware that the files are large and download times long. Use of the wget solution is recommended.

We have changed the algorithm for calculating indexes 008 and 009 (i.e. heat-wave days and warm-wave days) and now release corrected versions of these indexes in *Klimaatlas*, which are consistent with the calculations applied to DMI’s climatological data. This means that both data and figures are updated. Compared to the updated numbers, the previous method resulted in too many days being counted by several in the mean, and up to 12 days in some models.

We introduced a new bias-adjustment method of handling (low) extremes which influenced, to a small degree, indexes 301, 302, 401 and 402. New values for these were calculated and are part of version 2021a release. The change had to do with ensuring that small negative values are not produced during the bias-adjustment.

Two new sea level and storm surge indicators: frequency and accumulated duration of sea level exceeding current local warning level. The 10.000 year storm surge events are still subject to research, and an update is underway – read section 6.1.2 for details. We have changed the unit of the frequency of 20-year storm surge events to number of events per 20 year period.

The present data release, version 2021a, is identical to version v2020b, except for the indices 008, 009, 301, 302, 401 and 402 and the ocean information indexes 210, 211 and 212, which are updated.

Section 4 of the older versions of this report has been shortened and edited for clarity and the text therein now only details the procedures actually applied–see, e.g. version 20-20, for the older material.

9.4. Version v2020b, December 2020

With the update to version 2020b in December 2020, *Klimaatlas* has been expanded with 19 new indicators. The new data presents more details on the future changes in temperature, winds, evaporation, sunshine, frequent and rare storm surges.

Fourteen new atmospheric indicators: Daily high and low temperatures, maximum and minimum temperatures, annual and diurnal temperature intervals, heatwaves (hedebølger og varmebølger), frost days, growing season length, mean wind speed, number of storm events, potential evaporation, and solar radiation.

Five new sea level and storm surge indicators: 100- and 10,000-year storm surge events, 1and 5-year sea level events, and the change in frequency of current 20-year storm surge events.

The complete overview of the indicators in the current version of *Klimaatlas* can be found in Table 2.

The main updates to text concern calculation of new temperature indices (in Section 8) and the data for rare storm surge events (in Section 5).

9.5. Version v2020a, June 2020

With version v2020a, *Klimaatlas* has been updated to include 8 new indicators: the mean number of dry days, the mean duration for the longest dry period, and 5, 20, and 50 year events for hourly and daily precipitation. Furthermore, *Klimaatlas* is now based on data from more climate models; up to 57 models for daily values and 35 models for hourly values. Data for sea level and storm surges is unchanged since v2019a.

Note that some index numbers have changed since the previous version:the indices for2, 10, and 100-year events for hourly precipitation are now 151, 153, and 156 (previously 108, 109, and 110), and the indices for 2, 10, and 100-year events for 24-hour precipitation are now 157, 159, and 162 (previously 111, 112, and 113).

9.6. Version 2019a, October 2019

Klimaatlas was initially released on 6th October 2019 with 17 indicators:

- Precipitation
    - Average precipitation
    - Maximum daily, 5-day and 14 day precipitation
    - Days with more than 10-, and 20mm precipitation

  - Cloudburst frequency
  - 2-, 10-, and 100 year events for hourly precipitation
  - 2-, 10-, and 100 year events for daily precipitation
- Temperature
  - Average temperature
- Sea level and storm surge
  - Sea level rise
  - 20 and 50 year storm surge events

10. Appendix B Bootstrapping uncertainties

A data-product like *Klimaatlas* should not only give the magnitudes of numerical quantities, but also the uncertainties coupled to these quantities.

Cloudbursts, for instance, are likely under-observed since the events are small in extent and rare. Limited lengths of records have their main impacts through sampling of the climate variability: The climate system affecting Denmark has low-frequency variability and sampling such a sequence of data with limited-length windows causes a sampling issue: we may have samples from the real climate that are not representative of the mean climate. For instance, the North Atlantic Oscillation is a phenomenon influencing the track of low pressure systems in the North Atlantic. Therefore, temperatures, precipitation and winds over Denmark are dependent on the state of the NAO index. The influence of this is sampled by the limited availability of calibration-data.

At the moment, our understanding of the uncertainties is based on the spread provided by the models which we have available. Additional sources of uncertainty follow from the use of scope-limited observational material and from the use of interpolations and gridding techniques.

A good way to probe the relative importances of these sources of uncertainty, is to apply resampling of the data used, and re-parametrizations of the methods used. In 2019 we have employed resampling of observational data and the models used; in the future we will also probe the dependency on methods.

To perform the resampling of data we employ 'bootstrapping with replacement'. We apply the method to the years for which observational data exist, and for the models used. We do it separately so that the effects of these two important factors can be isolated.

The procedure is straightforward and is mainly one of repeating the calculation of *Klimaatlas* indices under random picks of years or models, followed by collation of results. We simply look at the spread - standard deviation - in the main result we report on: the 10, 50 and 90%-iles themselves. We report results for the end-of century period and for the RCP8.5 scenario, as we expect the largest effects there.

In Table 10 we show the standard deviations of the percentile levels reported on in this report (i.e. 10, 50 and 90). We are sampling local anomalies in order to exclude the considerable effect of geographic variations.

The Table is complex to interpret quickly and we have put it at the end of this report so that unwarranted confusion does not arise upon encountering the table in the main text. A brief explanation of what is in the table follows, but the reader mainly interested in following the flow of the text may wish to skip the rest of this paragraph: For each index, and for either bootstrapping observations (label S1 at head of column) or models (header S2 on column) we give 4 numbers — these are on two lines and each pair is separated by a semi-colon. On the first line and in front of the semi-colon is given the largest (i.e. 'worst-case') standard deviation of any of the percentiles 10, 50 and 90 for absolute values in the climate index. On the first line after the semi-colon is the largest standard deviation for any of the 10, 50 and 90%-iles of the change in the index. On the second line is given the same information as in the first line but now only for the median (i.e. the 50%-ile). We split the results in this way with the expectation that the effect on percentiles might not be the same for the 10, 50 and 90%-iles given small number statistics.

We did not apply bootstrapping on the climate indexes dealing with sea-levels and storm surges as the uncertainties there are given by error-propagating due to the limited number of sea level models currently available. In the future we could also probe the ocean-indices' uncertainties by resampling means.

So far, only 9 bootstraps have been performed, and only partially on factors S1 (observations) and S2 (models). However, these first results allow some general conclusions.

We see some differences in the effects of bootstrapping S1 (observation years) and S2 (models), respectively: For index 001 and 106, the effects due to bootstrapping on S1 and S2 are about the same for the absolute values and the climate signals in these (i.e. their changes over time). For indices 101-105 the standard deviation in the climate change signal is much bigger for S2 bootstrapping than it is for S1 bootstrapping.

For indices 107 and 151-162 we only have results for S2 bootstrapping. Here we note that the standard deviation on the climate signal for 151-162, due to S2 bootstrapping, is in the range 5-16%.

107 has very small response to bootstrapping, it appears.

Only minor differences are seen throughout when comparing standard deviations induced by bootstrapping for any of the percentiles 10, 50 and 90 when just considering the 50th percentile.

In summary:

- choice of models has greater influence than the choice of calibration period, by factors of from 4 to 10 (indices 101-105)
- uncertainties due to model choice can reach 16% in the change of indices related to extreme precipitation
- robustness of the 10, 50 and 90th percentiles to S1 (observation years) and S2 (models) bootstrapping are similar.

We should thus seek to extend the number of models used, and we should accommodate an analysis of the importance of calibration period position in time which could not be sampled by the present bootstrap analysis. More and longer observed data series should be obtained.

Extending the number of factors considered in bootstrapping could provide us with an important tool for calculating 'total uncertainty' on *Klimaatlas* information.

Indicator ID	Name of index	Units	S1 (obs)	S2 (mod)
001	Mean temperature	C C	±0.18 : ±0.13 ±0.18 : ±0.13	±0.16 : ±0.17 ±0.12 : ±0.12
101	Mean precip.	mm/day %	±0.13 : ±1.0 ±0.13 : ±0.9	±0.12 : ±5 ±0.09 : ±4
102	Daily-max precip.	mm %	±1.7 : ±0.6 ±1.7 : ±0.5	±1.6 : ±6 ±1.0 : ±4
103	5-day max precip.	mm %	±2.6 : ±0.86 ±2.5 : ±0.74	±2.0 : ±4 ±1.5 : ±3
104	14-day max precip.	mm %	±3.9 : ±0.9 ±3.8 : ±0.8	±4.5 : ±5 ±2.4 : ±4
105	Days with over 10 mm Daily precip.	days days	±0.7 : ±0.15 ±0.7 : ±0.13	±0.55 : ±0.57 ±0.43 : ±0.48
106	Days with over 20 mm Daily precip.	days days	±0.35 : ±0.12 ±0.35 : ±0.10	±0.20 : ±0.20 ±0.14 : ±0.15
107	Number of cloud-bursts per year	events events	- -	±0.074 : ±0.073 ±0.074 : ±0.073
151	Hourly precip. in 2-year events	mm %	- -	±0.90 : ±7 ±0.69 : ±6
153	Hourly precip. in 10-year events	mm %	- -	±3.0 : ±10 ±2.4 : ±9
156	Hourly precip. in 100-year events	mm %	- -	±8.6 : ±16 ±5.9 : ±13
157	Daily precip. in 2-year events	mm %	- -	±2.2 : ±5.3 ±1.7 : ±4.3
159	Daily precip. in 10-year events	mm %	- -	±4.9 : ±7.8 ±3.0 : ±5.4
162	Daily precip. in 100-year events	mm %	- -	±11.7 : ±11.4 ±5.8 : ±6.1

Table 6 Standard deviations in climate indexes, based on bootstrapping of local anomaly data (i.e. excluding the enhanced variability otherwise due to inclusion of geographic variations). Observation year and models are bootstrapped – labelled S1 and S2. Two pieces of information is given for each index - one is the absolute value of an index in the far future period 2071-2100, and the other is the change in that index between the far future period and the historical reference period. These two quantities are shown in each column before and after the semi-colon. The changes are either absolute (indexes 001, 105, 106 and 107), or are given as percentages. Values shown are for the scenario RCP8.5 and the distributions generated by the bootstrap include the various values from each bootstrap across the whole 1x1 km land-only grid of Denmark. 9 bootstraps were performed. For each index two lines are shown - the first line gives the largest standard deviation found in any of the 10, 50 and 90%iles - the second line is restricted to just the 50%ile (i.e., the median). The seasonal and the annual values are all included, except for index 107, which is annual only.